europhysicsnews

35/2
2004
March/April 2004
Institutional subscription price:
91 euros per year

FEATURES ISSUE

The art of taming light: ultra-slow and stopped light
Laser spectroscopy of nanometric gas cells
A new and exciting optically induced electron source
The quest for brilliance

features

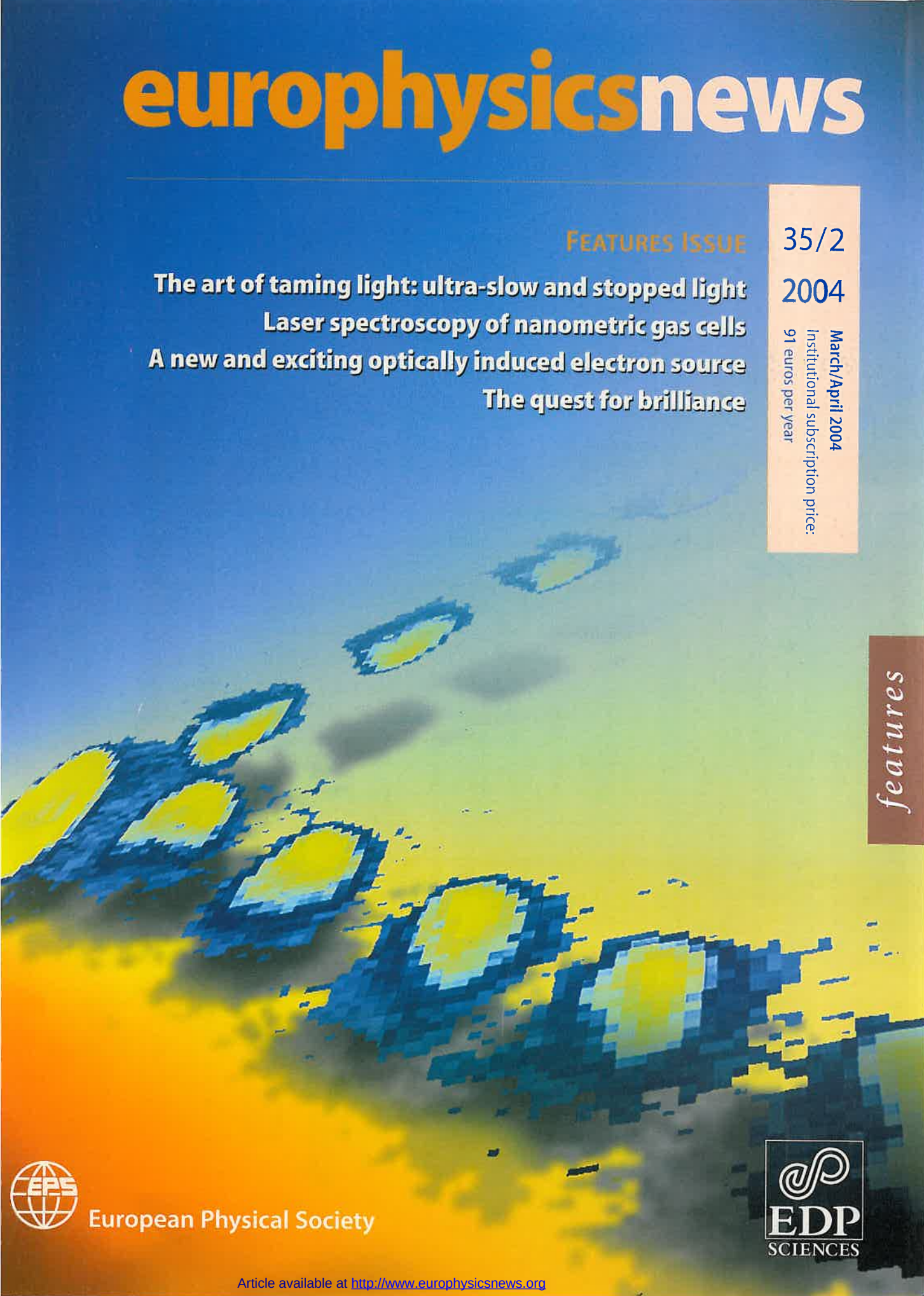

European Physical Society

EDP SCIENCES

2004 MRS FALL MEETING

Exhibit and research tools seminars

NOVEMBER 29–DECEMBER 3

BOSTON, MA

For additional meeting information, visit the MRS Web site at

www.mrs.org/meetings/

or contact:

MRS

Member Services
Materials Research Society
506 Keystone Drive
Warrendale, PA 15086-7573
Tel 724-779-3003
Fax 724-779-8313
E-mail: info@mrs.org

CALL FOR PAPERS

2004 MRS FALL MEETING

ABSTRACT DEADLINE JUNE 22, 2004

REMINDER: *In fairness to all potential authors, late abstracts will not be accepted.*

www.mrs.org/meetings/fall2004/

SYMPOSIA

ELECTRONICS, MAGNETICS, AND PHOTONICS

- A: Semiconductor Materials for Sensing
- B: Progress in Semiconductor Materials IV—Electronic and Optoelectronic Applications
- C: Innovations for Sub-100nm Lithography—Materials and Processes
- D: Materials and Processes for Nonvolatile Memories
- E: GaN, AlN, InN, and Their Alloys
- F: Group IV Semiconductor Nanostructures
- G: Materials, Integration, and Packaging Issues for High-Frequency Devices II
- H: Functional and Multifunctional Oxide Films
- I: Fabrication and New Applications of Nanomagnetic Structures
- J: Magneto-Optical Materials for Photonics and Recording

MATERIALS FOR ENERGY GENERATION AND STORAGE

- K: Solid-State Ionics
- L: Materials for Photovoltaics
- M: Materials Aspects of Fuel Cells
- N: Materials for Hydrogen Storage

ADVANCES IN MATERIALS CHARACTERIZATION

- O: Scanning-Probe and Other Novel Microscopies of Local Phenomena in Nanostructured Materials
- P: Electron Microscopy of Molecular and Atom-Scale Mechanical Behavior, Chemistry, and Structure
- Q: Neutron and X-Ray Scattering as Probes of Multiscale Phenomena

MECHANICAL BEHAVIOR

- R: Fundamentals of Nanoindentation and Nanotribology III
- S: Integrative and Interdisciplinary Aspects of Intermetallics
- T: Surface Engineering—Fundamentals and Applications
- U: Stability of Thin Films and Nanostructures
- V: Size Effects in Plasticity
- W: Mechanically Active Materials
- Y: Mechanical Properties of Bio-Inspired and Biological Materials

HYBRIDS AND SOFT MATTER

- Z: Bio-Inspired and Bio-Derived Materials and Processes
- AA: Applications of Micron and Nanoscale Materials in Biology and Medicine
- BB: Multicomponent Polymer Systems—Phase Behavior, Dynamics, and Applications
- CC: Liquid Crystal Materials and Technology
- DD: Organic and Nanocomposite Optical Materials
- EE: Organic/Inorganic Hybrid Materials

NOVEL MATERIALS FABRICATION AND APPLICATIONS

- FF: Solid-State Chemistry of Inorganic Materials V
- GG: Mesoscale Architectures from Nano-Units—Assembly, Fabrication, and Properties
- HH: Functional Carbon Nanotubes
- II: Modeling of One- and Two-Dimensional Nanomaterials
- JJ: Modeling of Morphological Evolution at Surfaces and Interfaces
- KK: Kinetics-Driven Nanopatterning on Surfaces
- LL: Materials Issues in Solid Freeforming
- MM: Ultrafast Lasers for Materials Science
- NN: Materials for Space Applications

MATERIALS TOPICS OF GENERAL INTEREST

- OO: Materials Issues in Art and Archaeology VII
- PP: Communicating Materials Science—Secondary Education for the 21st Century
- X: Frontiers of Materials Research—From Inception to Impact

MEETING ACTIVITIES

SYMPOSIUM TUTORIAL PROGRAM

Available only to meeting registrants, the symposium tutorials will concentrate on new, rapidly breaking areas of research.

EXHIBIT AND RESEARCH TOOLS SEMINARS

A major exhibit encompassing the full spectrum of equipment, instrumentation, products, software, publications, and services is scheduled for November 30–December 2 in the Hynes Convention Center, convenient to the technical session rooms. Research Tools Seminars, an educational seminar series that focuses on the scientific basis and practical application of commercially available, state-of-the-art tools, will be held again this fall.

PUBLICATIONS DESK

A full display of over 825 books, plus videotapes and electronic databases, will be available at the MRS Publications Desk.

SYMPOSIUM ASSISTANT OPPORTUNITIES

Graduate students planning to attend the 2004 MRS Fall Meeting are encouraged to apply for a Symposium Assistant (audio-visual assistant) position.

CAREER CENTER

A Career Center for MRS members and meeting attendees will be open Tuesday through Thursday.

The 2004 MRS Fall Meeting will serve as a key forum for discussion of interdisciplinary leading-edge materials research from around the world. Various meeting formats—oral, poster, round-table, forum and workshop sessions—are offered to maximize participation.

europhysicsnews

Volume 35 Number 2
March/April 2004

▲ PAGE 40

Laser spectroscopy of nanometric gas cells

▲ PAGE 47

From third to fourth generation light sources

▲ PAGE 50

Diffraction for industrial applications

FEATURES

NEWS, VIEWS AND ACTIVITIES

europhysicsnews

Europhysics News is the magazine of the European physics community. It is owned by the European Physical Society and produced in cooperation with EDP Sciences. The staff of EDP Sciences are involved in the production of the magazine and are not responsible for editorial content. Most contributors to Europhysics News are volunteers and their work is greatly appreciated by the Editor and the Editorial Advisory Board.
Europhysics News is also available online at: **www.europhysicsnews.com**

35/2
2004
March/April 2004
Institutional subscription price:
91 euros per year

Editor David Lee EMAIL: d.lee@uha.fr
Science Editor George Morrison EMAIL: g.c.morrison@bham.ac.uk
Designer Paul Stearn EMAIL: p.stearn@uha.fr
Directeur de la publication Jean-Marc Quilbé, EDP Sciences

Schedule
Six issues will be published in 2004. The magazine is distributed in the second week of January, March, May, July, September, November. A directory issue with listings of all EPS officials is published once a year.

Production and Advertising Agnes Henri
Address EDP Sciences,
17 avenue du Hoggar, BP 112,
PA de Courtabœuf,
F-91944 Les Ulis Cedex A, France
Tel +33 169 18 75 75
Fax +33 169 28 84 91

Printer Rotofrance, Lognes, France
Dépôt légal: mars 2004

Subscriptions
Individual Ordinary Members of the European Physical Society receive Europhysics News free of charge. Members of EPS National Member Societies receive Europhysics News through their society, except members of the Institute of Physics in the United Kingdom and the German Physical Society who receive a bimonthly bulletin. The following are subscription prices available through EDP Sciences. **Institutions** 91 euros (VAT included, European Union countries); 91 euros (the rest of the world). **Individuals** 58 euros (VAT included, European Union countries); 58 euros (the rest of the world). Contact subscribers@edpsciences.com or visit www.epdsciences.com

ISSN 0531-7479
ISSN 1432-1092 (electronic edition)

The art of taming light: ultra-slow and stopped light

Zachary Dutton[1,2], Naomi S. Ginsberg[2], Christopher Slowe[2], and Lene Vestergaard Hau[2]
[1] Lyman Laboratory, Harvard University, Cambridge MA 02138
[2] Present address: National Institute of Standards and Technology, Electron and Optical Division, Gaithersburg MD 20899-8410

In 1998, laser pulses were slowed [1] in a Bose-Einstein condensate (BEC) [2] of sodium to only 17 m/s, more than seven orders of magnitude lower than the speed of light in vacuum. Associated with the dramatic reduction factor for the light speed was a spatial compression of the pulses by the same large factor. A light pulse, which was more than 1 km long in vacuum, was compressed to a size of ~50 μm, and at that point was completely contained within the condensate [1]. This allowed the light-slowing experiments to be brought to their ultimate extreme [3]: in the summer of 2000, light pulses were completely stopped, stored, and subsequently revived in an atomic medium, with millisecond storage times [4]. The initial ultra-slow light experiments spurred a flurry of slow light investigations, and slow or partially stopped light has now been observed in limited geometries in warm rubidium vapours [5-7], liquid-nitrogen cooled crystals [8], and recently in room temperature crystals [9].

Here, we begin with a discussion of ultra-slow and stopped light. We describe how cold atoms and Bose-Einstein condensates have been manipulated to generate media with extreme optical properties. While the initial experiments concentrated on the light propagation, we have recently begun a number of investigations of the effects that slow light has on the medium in which it propagates. Effects are profound because both the velocity and length scales associated with propagating light pulses have been brought down to match the characteristic velocity and length scales of the medium. With the most recent extension, the *light roadblock* [10], we have compressed light pulses to a length of only 2 μm. Here, we describe the use of ultra-compressed light pulses to probe superfluidity and the creation of quantized vortices in BECs through formation of 'superfluid shock waves'.

We also present the observation of an ultra-slow-light-based, pulsed atom laser. Furthermore, we demonstrate the use of slow and stopped light for manipulation of optical information, in particular in Bose-Einstein condensates that allow for phase coherent processing of three-dimensional, compressed patterns of stored optical information.

Ultra-slow light

In our experiments we use a cloud of ultra-cold sodium atoms, trapped by an electromagnet in an ultra-high vacuum chamber (Fig. 1a). By illuminating the cloud with a precisely tuned 'coupling' laser beam, the optical properties of the atoms can be dramatically altered so that a laser pulse, subsequently sent through this coupled atom-light medium, will move at very low velocity. By choosing the right polarisations of the two laser beams, the light fields selectively couple three internal energy levels of the atoms (Fig 1b).

Initially, the atoms are all in the ground state labeled $|1\rangle$, and the laser fields are off. The coupling laser is turned on and couples $|2\rangle$ to the upper state, $|3\rangle$. Since $|2\rangle$ is unpopulated, the coupling laser is not absorbed but rather causes the upper energy level, $|3\rangle$, to split symmetrically into two new energy levels (Fig. 1b). The energy difference between these new states is proportional to the magnitude of the electric field of the coupling laser. A 'probe' light pulse, tuned to the $|1\rangle$-$|3\rangle$ transition, is injected into the BEC. It is this light pulse that is compressed and propagates at ultra low group velocity. A light detector (PMT in Fig. 1a) is used to measure the arrival of the pulse as it exits the atom cloud.

The refractive index profile for the probe pulse in the slow-light medium is shown in Fig 1c. The refractive index on resonance is unity—the value in free space—because the contributions to the susceptibility from the two symmetrically split energy levels exactly cancel. This results in a steep and linear refractive index variation around the $|1\rangle$-$|3\rangle$ resonance, which leads to low light speeds since the signal velocity of a light pulse is inversely proportional to the refractive index *slope*. With cold atoms there is a negligible Doppler smearing of the energy levels and illumination with very low coupling intensities is possible. This brings the split levels close together and creates very steep refractive index slopes and extremely low light speeds. While the pulse is in the atom cloud, its group velocity and spatial extent are both proportional to the intensity of the coupling field and inversely proportional to the atom density. These parameters can be experimentally controlled.

A resonant probe pulse would be completely attenuated in the atom cloud in the absence of the coupling laser. However, when the coupling laser is present, a narrow transmission window is created around resonance, and the pulses can propagate though the atom cloud. This effect, electromagnetically induced transparency [11], is also responsible for maintaining the very steep slopes of the refractive index profile, even in the presence of spontaneous radiation damping from the upper state, $|3\rangle$, which would otherwise broaden the profile in Fig. 1c. It occurs due to a quantum mechanical interference created in the atom-light system: absorption of a probe photon is associated with the transition of an atom from $|1\rangle$ to $|3\rangle$. However, there is another path to that final state, where the atom absorbs a coupling photon and makes a transition from $|2\rangle$ to $|3\rangle$. As a result, when the atom is in a very particular quantum mechanical superposition of $|1\rangle$ and $|2\rangle$, the transition amplitudes for the two paths cancel. In this 'dark state', the atom absorbs from neither the probe nor the coupling laser fields, and the amplitude for the atom to be in $|2\rangle$ relative to the amplitude for $|1\rangle$, A_2/A_1, is proportional to minus the ratio of the electric field amplitudes of the probe and coupling laser fields. This makes the process phase sensitive: the ratio A_2/A_1 is a complex number that depends on the relative phase of the probe and coupling fields.

As the light pulse enters the atom cloud, the front edge slows down, the back edge—still in free space—catches up and the pulse spatially compresses. As the pulse propagates through the atom cloud, the atoms within the spatially localized pulse region are in dark superposition states. The spatial distribution of the dark states mimics the spatial variation of the light pulse: the pulse makes an imprint—a hologram, really—in the atom cloud and this imprint follows the pulse as it slowly propagates. Eventually the light pulse and the imprint reach the other end of the cloud where the front edge speeds up and the pulse expands spatially. The light pulse reaches the same shape as it had before it entered the medium, but is delayed by several microseconds in a cloud of only 100-200 μm (Fig 1d).

Fig. 2a shows images of the atomic imprint of a 2 μs light pulse, with a length of 600 m in free space, as it compresses and propagates into a 100 μm long and 30 μm wide, cigar-shaped

Bose-Einstein condensate. To photograph the pulse, we selectively image $|2\rangle$ atoms in the cloud with the 'imaging' laser beam shown in Fig.1a, revealing the instantaneous shape of the imprint. The transverse width of the probe laser beam (in the *x*-*y* plane) is larger than the size of the condensate. The pulse is entering the cloud, and compressing, through the first 5 μs and then starts its slow propagation into the cloud. The observed boomerang shape of the light pulse (at 5 μs) reflects that the light speed along the centreline of the condensate is significantly lower than at the edges due to the high atom density in the middle of the cloud.

Stopped light

Because of the aforementioned spatial compression, the light pulse is eventually completely contained within the atom cloud. By an abrupt turn-off of the coupling laser, the moving light pulse stops and turns off, but leaves the holographic imprint frozen in the cloud [4]. Figure 2b shows a light-stopping experiment performed in a Bose-Einstein condensate, with two probe light pulses incident on the condensate from opposite directions. The light pulses are stopped in the atom cloud just before they collide, resulting in an imprint with a double boomerang shape (0 ms). Because of photon-induced recoils, that come from the coherent transfer of atoms from $|1\rangle$ to $|2\rangle$, the two 'boomerangs' are shot out at ± 45°, each with a velocity of 4.2 cm/s. This shows very directly that the process is coherent: to reach $|2\rangle$, the atoms absorb a probe photon and emit a coupling photon through *stimulated* emission. If instead, $|2\rangle$ had been reached via spontaneous, incoherent emission from $|3\rangle$, the two ejected atom clouds would (on average) have been kicked out along the ±*z*-directions and would have had a velocity spread comparable to the recoil velocity.

Since the slow-light and light-storage process is coherent, the ejected imprints are small condensates of $|2\rangle$ atoms. The observed changes in shape of the imprints as a function of time, as shown in Fig 2b, are indeed in agreement with calculations of condensate dynamics, based upon mean-field theory [12]. In effect, we have created a pulsed atom laser with a controllable spatial mode and a well-defined output-coupling velocity. Such an ultra-slow-light-based atom laser could be used as a source for a high-brightness atom interferometer. Such interferometers are beginning to rival classical precision measuring devices including navigational gyroscopes [13] and gravitometers [14].

We have also studied the case of stopped light for co-propagating coupling and probe laser beams with opposite circular polarisations. In this case, photon-recoil effects are negligible, and atoms in $|2\rangle$ are trapped by the electromagnet similarly to atoms in $|1\rangle$. The holographic imprint of the stopped light pulse therefore stays in the cloud for a long time. By switching the coupling field back on, the amplitude and phase of the atomic wavefunctions are written back onto the probe field, and the light pulse is revived after a long storage time in the medium.

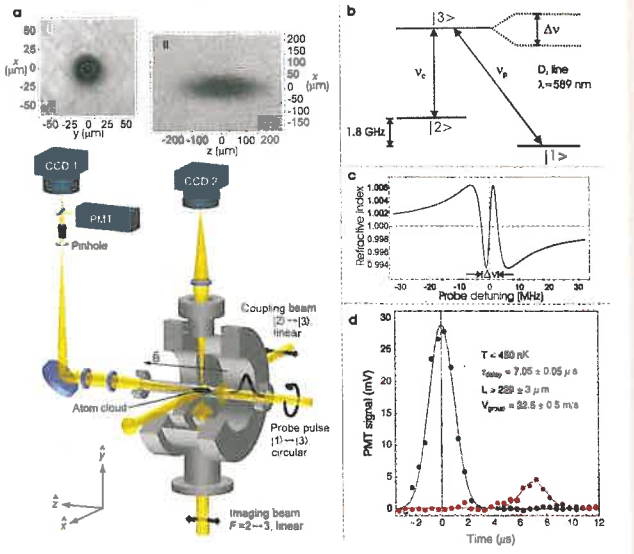

▲ **Fig. 1: Ultra-Slow Light**

(a) Experimental setup for generating slow and stopped light (from ref. 1). The cigar-shaped, cooled atom cloud, consisting of sodium atoms in state $|1\rangle$ (see (b)), is typically 100-200 μm long and is trapped in an electromagnet. The cloud is first illuminated from the side (along *x*) by a coupling laser beam. The intensity and frequency of this illuminating laser control the optical properties—in particular, the refractive index profile and the transmission—for a probe laser pulse subsequently sent into the medium (along *z*). This light pulse then propagates extremely slowly through the atom cloud. For propagation in a BEC, we obtain, with low coupling laser power (12 mW/cm²), a light speed of only 17m/s. The condensate would be completely opaque in the absence of the coupling field, but the presence of this laser field allows transmission of the light pulse (electromagnetically induced transparency). A photo-multiplier tube (PMT) is used to measure the delay and transmission of a probe pulse. The size of the atom cloud is determined with use of a third laser, the 'imaging beam'. This laser beam is sent into the system from below (along *y*) and the absorption shadow of the atom cloud, created in the beam, is recorded on a CCD camera (CCD2). An example is shown in inset (ii). Another camera, CCD1, is used to image the cloud in the x-y plane. For the slow and stopped light experiments (Figs 1 and 3), a pinhole is placed in an external image plane so the PMT detects light only that has been transmitted through the central 15 microns of the condensate (indicated by the dashed circle in insert (i)).

(b) Three-level (Λ) system of internal atomic states used to create slow light. The probe and coupling laser beams are resonant with the $|1\rangle$-$|3\rangle$ and $|2\rangle$-$|3\rangle$ transitions, respectively, and couple the three states. Here, ν_p and ν_c represent the resonance frequencies, and Δν is the distance between the new split energy levels of the atom/coupling-laser medium. Through the choice of frequencies and polarisations for the probe and coupling lasers, we control which atomic states participate in the process. The states used for the ultra-slow light measurement in (d), obtained with the polarisations indicated in (a), are $|1\rangle=|3S,F=1,M_F=-1\rangle$, $|2\rangle=|3S,F=2,M_F=-2\rangle$, and $|3\rangle=|3P_{3/2},F=2,M_F=-2\rangle$.

(c) Refractive index profile. We show the refractive index for the probe laser as a function of its detuning from the $|1\rangle$-$|3\rangle$ resonance frequency. Note that the refractive index on resonance is unity, the value in free space. Importantly, the refractive index has a very steep slope around resonance, and since the group velocity of a light pulse is inversely proportional to that slope, the profile shown leads to ultra-slow light. The figure was obtained for a coupling intensity of 12 mW/cm² and an atomic density of $3.3\cdot10^{12}$/cm³.

(d) Observation of ultra-slow light (ref. 1). The blue data points represent a reference pulse recorded with no atoms in the system and used to set the zero-point for the time axis. The red data points show a pulse that has propagated through an atom cloud cooled to 450 nK which is just above the transition temperature for BEC (the peak atomic density, in the cloud centre, is $3.3\cdot10^{12}$/cm³). In this case the delay of the light pulse is 7 μs, in a cloud that is only 229 μm long (see insert (ii) in (a)). This results in a light speed of 32 m/s which is seven orders of magnitude below the value in free space.

Fig. 3a shows a slow-light measurement with this setup, performed in a cold atom cloud cooled to 900 nK (which is just above the transition temperature for Bose-Einstein condensation). The pulse delay is 12 μs, and the arrow indicates the point in time when the light pulse is slowed, compressed, and totally contained in the middle of the atom cloud. In Figs 3b-c we abruptly turn the coupling laser off at this time and freeze a holographic imprint in the cloud. Since the imprint contains all the amplitude and phase information of the original light pulse, we can later revive the light pulse and send it back on its way, by simply turning the coupling laser back on. The storage times for the light pulse are 38 μs (Fig. 3b) and 833 μs (Fig. 3c), respectively.

The revived light pulses can also be manipulated [4]. In Figs 3d-e, a single light pulse is stored in the atom cloud and later regenerated in two (Fig. 3d), and even three, small pieces (Fig. 3e) by switching the coupling laser on and off several times. Furthermore, we have observed that by turning the coupling laser back on at a higher (lower) intensity, a temporally shorter (longer) light pulse can be regenerated. In the language of optical engineering, the bandwidth of the system can be manipulated dynamically, even for Fourier transform limited pulse propagation.

The storage times for compressed optical information are limited due to thermal smearing of the stored imprints, and are optimised with the ultra-cold clouds we are using. For the parameters in Figs 3, the storage time was limited to a few milliseconds.

Coherent processing of optical information

This storage time can be increased dramatically with optical storage in Bose-Einstein condensates, which are phase coherent objects. Furthermore, the dynamics of the condensates during the storage time can be utilised for processing of the stored optical information. The dynamics change the spatial structure of the ground state coherences—the dark states—leading to regenerated probe pulses with amplitude and phase changes that reflect the dynamics.

We have developed a comprehensive formalism to study these effects [15,16] and examples are shown in Fig. 4. Storing a slowed light pulse in a BEC creates a two-component condensate, a mixture of $|1\rangle$ and $|2\rangle$ atoms. The ensuing dynamics include nonlinear atom-atom interactions between the two condensate components. Our formalism, based on self-consistent Maxwell and condensate mean-field equations, describes a two-component BEC exposed to coupling and probe laser fields.

In Fig. 4a, the condensate component of $|1\rangle$ atoms creates a mean-field repulsive potential for the component of $|2\rangle$ atoms. The sum of the magnetic trapping potential and this mean field forms an effective potential with sharp edges. The $|2\rangle$ condensate reflects off this boundary, which leads to formation of interference fringes in the density of $|2\rangle$ atoms. Remarkably, by subsequent turn-on of the coupling laser, these complicated structures are written, with high fidelity, onto a revived probe pulse (Fig. 4b).

Unlike the above example, which utilises a weak probe field, a different regime is represented by Figs 4c-d where a strong probe pulse, of about the same peak electric field amplitude as that of the coupling field, propagates into a condensate and is stored (Fig. 4c). In this case, the slow-light and storage process significantly changes the density of both condensate components, and this leads to strong nonlinearities in the condensate dynamics. In Fig. 4d (left), the two components are seen to phase-separate, and two dark solitons are spontaneously formed in the condensate of $|1\rangle$ atoms, with

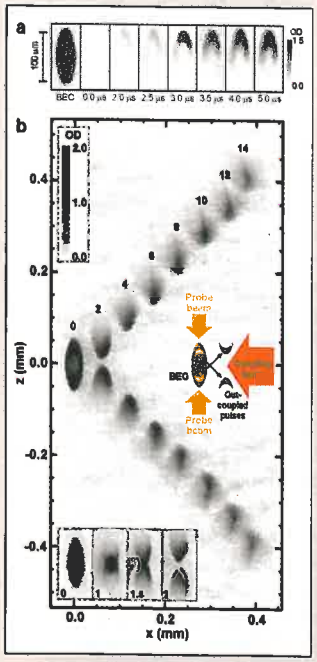

▶ **Fig. 2: Atom Laser with Ultra-Slow and Stopped Light**
(a) Observation of the slow-down and spatial compression of a light pulse in a BEC. Setup is as in Fig 1a. The first figure ('BEC') shows a condensate of $|1\rangle$ atoms, imaged before the light pulse is sent in. The picture is taken with the imaging beam and recorded on CCD2. The condensate is subsequently illuminated with the coupling laser and the probe light pulse is sent into the atom cloud. As described in the text, within the light pulse region, the atoms are in coherent dark states that are superpositions of $|1\rangle$ and $|2\rangle$. The spatial distribution of the dark states mimics the spatial shape of the light pulse. This atomic imprint, created by the light fields, travels with the light pulse. By selectively imaging the density of atoms in $|2\rangle$ (on CCD2), we can thus image the light pulse as it propagates through the condensate. The following pictures (from 0 μs to 5 μs) show such images of the light pulse as it propagates into the atom cloud and spatially compresses. At 0 μs, we start inputting the front edge of the light pulse. After 5 μs, the pulse is fully input, compressed, and totally contained within the cloud. The pulse starts out in free space, with a Gaussian shape and a length of 1 km, and is compressed in the condensate to only 25 μm. The light pulse is also seen to develop a 'boomerang' shape. The probe laser beam is uniform across the cloud in the *x*-direction (in the *y*-direction, the beam is only 20 μm wide to minimize smearing of the pulse shape in the images), and in the middle of the condensate, where the atom density is high, the pulse travels significantly slower than at the edge of the cloud, where the density is low, creating the boomerang shape. The grey-scale indicates the on-resonance optical density (OD) of the images, obtained as minus the natural logarithms of the transmission coefficient.
(b) Atom laser. For this experiment we send two counter-propagating probe light pulses into a Bose-Einstein condensate where they are stopped and form the double-boomerang imprint in the cloud labeled '0'. (The numbers in the figure indicate the times, in milliseconds, after the light pulses are input and stopped). Again, we selectively image the density of $|2\rangle$ atoms. To reach $|2\rangle$, the atoms have absorbed a probe photon and, through stimulated emission, emitted a coupling photon, leading to a $\pm 45°$ photon-induced recoil of the $|2\rangle$ atoms. We clearly see the two recoiling, boomerang-shaped imprints of $|2\rangle$ atoms as they are kicked out of the condensate (2-14 ms) with a velocity of 4.2 cm/s. They cross at 1 ms as shown in the inset. At 2 ms, the imprints are separated again but still maintain their boomerang shape. Since the slow-light and storage process is fully coherent (as confirmed by the recoil directions), and the atom imprints are output-coupled from a condensate, the ejected atom clouds are condensates of $|2\rangle$ atoms. This is confirmed by studying the ensuing dynamics. The associated shape changes as a function of time agree with a Gross-Pitaevskii mean-field description [12] of condensate dynamics. Between the boomerang arms, a narrow 'snout' of atoms forms, which is clearly seen sticking upward (on the upper track) at 10 and 12 ms. This sharp feature is due to an interference between atoms moving inward from the two boomerang arms. With this setup, we have created a pulsed atom laser with spatially controlled output coupling. In the case shown, there are 5 million atoms in the initial condensate of $|1\rangle$ atoms, and each output coupled condensate of $|2\rangle$ atoms contain 225,000 atoms.

the associated density dips filled by $|2\rangle$ atoms. (Solitons are excitations that maintain their shape due to a perfect balance between dispersion of collective excitations and nonlinear atom-atom interactions. Dark solitons give rise to a depletion of the atom density [17] as opposed to bright solitons where the density is enhanced). The result is extremely stable, filled 'vector solitons' [18,19]. Due to phase gradients in the condensate, the vector solitons move around and interact with each other. Upon subsequent pulse revival, the relative amplitude and phase of the two-component condensate, including the solitons, are written onto and transferred to the light fields (Fig 4d, right panel). We see that in this strong probe case, the coupling light field is also strongly affected by the atom dynamics.

It is now clear that by controlling the coupling beam parameters, the shape and size of the outgoing probe pulses can be manipulated, and mapping between atomic and light media can be performed with high fidelity [15]. In the weak-probe limit and for certain atom-atom interaction parameters, the $|2\rangle$ atoms experience, during the storage time, a predictable trapping potential with its own set of eigenstates. By choosing an incoming probe pulse profile that corresponds to one of these eigenstates, the amplitude of the stored imprint is stationary, and the imprint will evolve purely in phase. This setup could form the basis for a one-bit phase shifting gate. If the initial pulse is not a pure eigenstate of the system, as in Fig. 4a, it can be represented by a superposition of eigenstates that will evolve independently and lead to deterministic reshaping of the revived light pulse. Inputting stronger probe pulses leads to nonlinear evolution in the condensate which can be used for nonlinear processing of pulses. For example, one could input two spatially separated light pulses and the ensuing evolution will cause them to interact and introduce additional phase shifts on each other. This is the ingredient necessary to construct a two-bit conditional phase gate—a fundamental building block of quantum (or optical) computation. Furthermore, atom-atom interactions can be controlled with external electric and magnetic fields [20,21], with the exciting potential for dynamically controlled processing of stored optical information.

Following the storage of a classical light pulse in a BEC, condensate dynamics could develop non-classical entangled-atom states [22,23]. By subsequently reviving the light pulse [24], we could generate non-classical light fields from purely classical input fields. The storage and revival of non-classical light fields, with controlled processing during the storage time, as described above, could be of great importance for quantum information processing where the transfer between flying qubits (photons for example) and stationary storage devices (atoms for example) is of paramount importance [25].

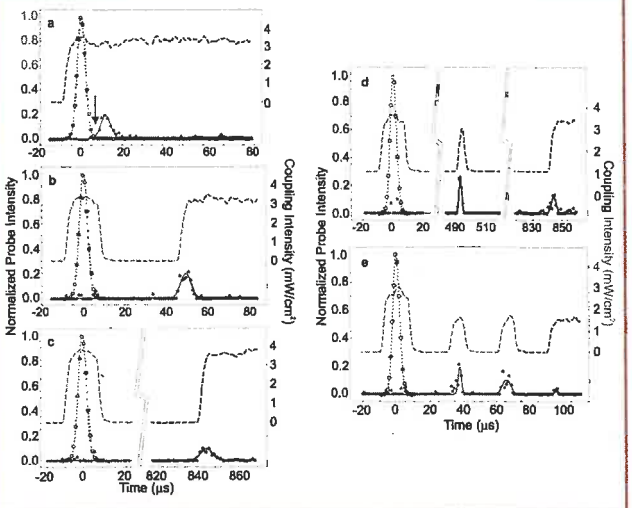

▲ Fig. 3: Stopped Light

(a) Slow light pulse observed as in Fig. 1d. However, in this case, the probe and coupling lasers are co-propagating and have opposite circular polarisations. The Λ system here has $|2\rangle=|3S,F=2,M_F=+1\rangle$ and $|3\rangle=|3P_{1/2},F=2,M_F=0\rangle$. There is no photon recoil and both $|1\rangle$ and $|2\rangle$ are trapped by the magnet ($|1\rangle$ and $|2\rangle$ have opposite gyromagnetic ratios). In the figure, open circles represent a measured reference pulse, and solid dots represent a pulse measured after it has been delayed by 12 μs in a cold cloud (900 nK with peak density $10^{13}/cm^3$). The dashed curve shows the intensity of the coupling laser which is turned on just a few microseconds before the probe pulse is sent in. The arrow indicates the point in time when the pulse is slowed, compressed, and contained in the middle of the cloud.

(b-c) Observation of stopped light. At the point in time indicated by the arrow in (a), we abruptly turn off the coupling laser, with the result that no probe pulse emerges. Some 38 μs later (b), we turn the coupling laser back on, and a light pulse is observed, with the same shape and intensity as measured in (a). Clearly, in this case, we have stopped the pulse and later revived it. In (c) we perform the same experiment as in (b) except we store the imprint in the cloud for 833 μs before we revive the light pulse.

(d-e) Manipulation of stored optical information. Here we inject and stop a single light pulse in the atom cloud. By switching the coupling laser on and off several times, we regenerate the light pulse in two small pieces (d) and even in three small pieces (e). The probe pulse intensity in the figures is normalised to the peak intensity of the reference pulse. Figs (a-e) are from ref. 4.

The light roadblock and superfluid dynamics

We now turn our attention to the description of how slow light can be used for direct probing of superfluid properties of Bose-Einstein condensates. By spatial modulation of the coupling laser intensity along the propagation direction of the probe pulses [10], we can, for example, control the speed and spatial extent of light pulses as they are propagating through the atom cloud. By spatially cutting off the coupling laser in the middle of the condensate, we form a *light roadblock*: a probe pulse slows down and compresses dramatically as it is running into the region of very low coupling intensity (Fig. 5a). With this method, light pulses 1 km-long in free space are compressed to 2 μm in a Bose-Einstein condensate. Within the localised pulse region at the roadblock, the atoms are driven almost entirely into $|2\rangle$ (the dark state when the coupling intensity goes to zero). As discussed above (Fig. 2b), the localised 'defect' of $|2\rangle$ atoms is kicked out of the magnet in less than a millisecond, due to photon recoil.

In the electromagnet, we are thus left with a $|1\rangle$-atom condensate with a slice punched in the middle. This void is so localised that it is comparable to the condensate's healing length, the length over which a superfluid can adjust to external perturbations [26]. The density depletion of the condensate breaks into two density dips that move at the local sound speed towards the condensate boundaries. Since the density defects are narrow and deep, nonlinearities from atom-atom interactions lead to a steepening of their back edges during propagation in the condensate, which results in 'quantum shock waves' [10], the superfluid analogue of shock waves in a classical fluid.

An experimental observation of this process is shown in Fig. 5b (from ref. 10). A narrow density defect is created at the light roadblock, which immediately leads to formation of dark solitons (white stripes at 0 ms). However, the solitons are unstable and their fronts

start to curl up, as seen at 0.5 ms. Subsequently, the points along the main front, with the largest curvature, act as nucleation sites for vortices with quantized circulation [26]. Vortices are observed at 2.5 ms and are seen as white 'dots' where the condensate density vanishes. Quantized vortices are very stable excitations of the superfluid condensate. They are clearly seen at 11 ms, for example.

By means of shock-wave formation, vortices are created far out of equilibrium, in pairs of opposite circulation, like particle anti-particle pairs. Changing the length and intensity of a light pulse sent towards the light roadblock adjusts the number of vortices formed. Hence, we can controllably form many-body systems of vortices and study their collision dynamics: in some cases the vortices collide like billiard balls, in other cases their collisions lead to annihilation and the energy is released in the form of outgoing sound waves.

An example is shown in Fig. 6a, which is the result of a numerical simulation of vortex dynamics in two dimensions, for realistic experimental parameters. After a narrow defect is created at the light roadblock, a total of 12 vortices are nucleated (11 ms). Examination of the phase pattern of the condensate wavefunction reveals that the vortices are singly quantized. They are created in pairs of opposite circulation, with each vortex pair located at opposite sides of the horizontal symmetry axis ($x=0$). The three vortices in each quadrant spin around each other due to the velocity fields of adjacent vortices, two out of each triplet annihilate, and the energy is carried off as sound waves (seen as curved fronts at 16.5 ms and 17.5 ms).

There are then four long-lived vortices remaining. The vortices first move towards the condensate edge, scatter, and circle back towards the centre, which puts them on a collision course. At 57 ms they collide and their paths make a sharp 90° turn. The vortices then circle back after colliding with the condensate boundaries, and a second collision occurs after 122 ms, which gives rise to a sound wave (the curved fronts at 123 ms) that is seen emanating from the centre.

We should be able to create a controlled many body system of these 'vortex particles' as illustrated by the calculation shown in Fig. 6b. Here, a light pulse, stopped at a light roadblock in a pancake shaped BEC, causes a whole line of vortices to form on both sides of the condensate. With the addition of a third dimension, vortex rings and filaments replace these vortex point particles and introduce a

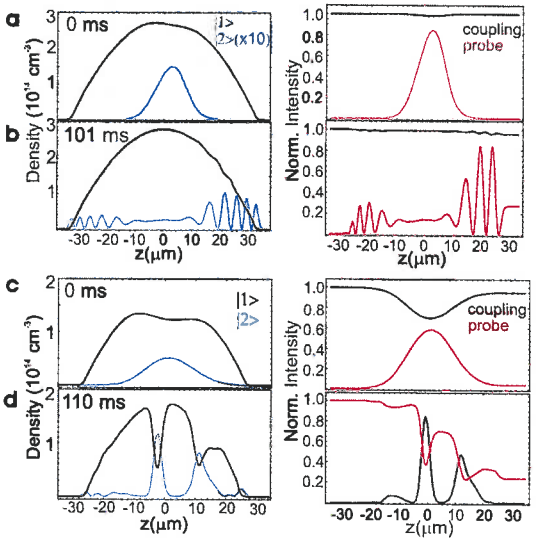

▲ Fig. 4: Coherent Processing of Optical Information
The calculations are performed for ^{87}Rb (note that all other figures are for sodium). Rubidium has scattering rates, for inelastic scattering between the hyperfine ground states $|1\rangle$ and $|2\rangle$ (of the Λ system), that are lower than those in sodium by two orders of magnitude [30]. Rubidium is therefore particularly well suited for coherent processing over long time scales.
(a-b) Weak probe case. A probe pulse is injected into a BEC under ultra-slow-light conditions and subsequently stopped in the condensate (at 0 ms). The corresponding densities of $|1\rangle$ (black) and $|2\rangle$ (blue) condensate atoms are shown in the left panel of (a). Coherent two-component condensate dynamics, with atom-atom interactions playing a major role, will effectively process the stored light pulse information. In the example shown here, the condensate component of $|2\rangle$ atoms will scatter off the sharp potential edge formed by the magnetic trapping potential in combination with the repulsive mean-field potential from the $|1\rangle$ component. The reflected condensate component interferes with itself and forms interference fringes in the density of $|2\rangle$ atoms (b). The right panels show the results of switching the coupling laser back on at 0 ms and at 101 ms, respectively. Remarkably, the complicated interference pattern in the $|2\rangle$ condensate is written onto the probe light field with high fidelity (the red curve represents the probe intensity normalised to the peak intensity of the input pulse). The coupling intensity (normalised to the input intensity and shown as the black curve) is hardly affected.
We use co-propagating probe and coupling laser beams with opposite circular polarisations such that the states forming the Λ system are $|1\rangle=|5S,F=2,M_F=+1\rangle$, $|2\rangle=|5S,F=1,M_F=-1\rangle$, and $|3\rangle=|5P_{1/2},F=2,M_F=0\rangle$. Dictating this choice was our desire for a particular relationship between the scattering strengths for the different condensate components, which control the processing. Here, the s-wave scattering length for collisions between $|2\rangle$ atoms is $a_{22}=5.36$ nm, and the ratios between this quantity and the scattering lengths for collisions between $|1\rangle$ atoms and between $|1\rangle$ and $|2\rangle$ atoms are $a_{11}:a_{12}:a_{22}=0.95:0.975:1$. There is no photon-induced recoil, and both condensate components are trapped by the magnet.
(c-d) Strong probe case. This represents a different regime, where the probe and coupling laser strengths are comparable. This leads to significant nonlinear effects in the condensate dynamics, and associated nonlinear processing of optical information is possible. When a probe light pulse is input and stopped in the condensate (0 ms), a large fraction of the atoms within the pulse region are transferred to $|2\rangle$. The corresponding depletion of the condensate of $|1\rangle$ atoms is significant and influences the ensuing two-component condensate dynamics, leading to the nonlinearities. In this case, the two components phase-separate: the $|1\rangle$-condensate component develops two dark solitons filled with state $|2\rangle$ condensate atoms. The resulting density in the two components, after 110 ms of evolution, is shown in (d), left panel. The coupling laser is switched on at this time, and the revived probe pulse is shown in the right panel (red curve). As is seen, the solitons are written onto the probe light field. In this strong-probe case, the coupling laser is significantly affected by the write process, and it is really in the ratio of the two light field amplitudes that the full result of the processing is contained. The solitons correspond to large phase gradients in the condensate wavefunction, and these phase gradients are also written onto the light fields [15].
For these calculations, we used co-propagating probe and coupling laser beams with opposite circular polarisations, but now with frequencies of the laser fields tuned such that the states of the Λ system are $|1\rangle=|5S,F=1,M_F=-1\rangle$, $|2\rangle=|5S,F=1,M_F=+1\rangle$, and $|3\rangle=|5P_{1/2},F=2,M_F=0\rangle$. The scattering lengths are $a_{11}=a_{22}=5.36$ nm, and $a_{12}=1.04\,a_{11}$. The latter is larger than the value for an isolated rubidium atom where $a_{12}=1.005\,a_{11}$. The larger value is chosen in order to speed up the processing. Scattering lengths can be controlled with external electric and magnetic fields.

host of new and exciting dynamics as a result of the more complicated topology.

Spatial modulation of the coupling laser [10] in a slow light medium forms the basis for the proposed observation of effects of general relativity in table-top, earth-based experiments [27], and for recent photonic bandgap induced storage of light pulses in atomic media [28].

Outlook

As described above, ultra-slow light allows for the ultimate control of light: the manipulation, storage, and processing of optical information. We imagine that ultra-slow light can be used as a basis for creating dynamically controllable optical delay lines with large and variable optical delays obtained in very small optical structures. The delays and the bandwidth of such a system could be controlled simply through control of the coupling laser intensity. It is important to note, that temporal spreading, spatial distortion, and absorption are all minimised for light-pulse propagation under ultra-slow light conditions because of the linear variation of the refractive index with frequency around its unity value at resonance.

The dramatic spatial pulse compression and coherent, holographic imprinting of optical information in atomic media, associated with ultra-slow light, led to the observation of stopped light. Using this technique, we envision developing three-dimensional optical storage devices with optical information stored in highly compressed form, and the creation of optical shift registers controlled by the on/off switching of a coupling laser with illumination in spatially selected regions. Dynamical bandwidth control for transform limited pulse propagation is possible, as is controlled coherent processing of optical information through utilisation of the coherent dynamics of Bose-Einstein condensates. Furthermore, ultra-slow-light-based output-coupling from condensates of very localised coherent structures with controlled spatial shapes and recoil

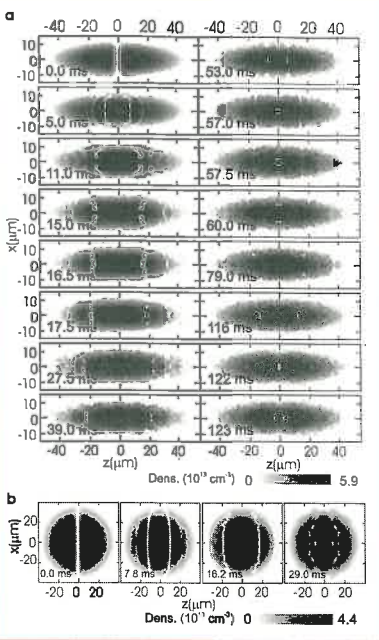

Fig. 6: Quantum Shock Waves and Vortex Dynamics
(a) Vortex dynamics. A numerical calculation of the dynamics for a sodium condensate after a deep, narrow density defect has been created at *t=0* at a light roadblock. The dynamics are calculated with the non-linear Gross-Pitaevskii equation [12], and the plots show the density of the condensate at the times indicated. The formation, dynamics, and interactions of the vortices formed by the defect are discussed in the text. The size and amplitude of the defect is controlled with the duration and intensity of the probe pulse and in this case, a 100 % density defect, with a half-width of 3 μm, is imposed initially, and this leads to formation of 4 long-lived vortices that first collide like billiard balls (at 57 ms) and then scatter off the condensate boundaries. A second collision (at 122 ms) results in the creation of a large spherically outgoing sound wave (123 ms).
(b) Many-body system of vortices. Numerical calculation of the dynamics for a condensate, trapped in a spherically symmetric magnetic field, after a defect with half-width 2.3 μm is imposed. We see that the deepest solitons break up into ten vortices each. The number of vortices formed is determined by the intensity and duration of the probe pulse, and the light roadblock is therefore ideal for controlled studies of many-body systems of vortices.

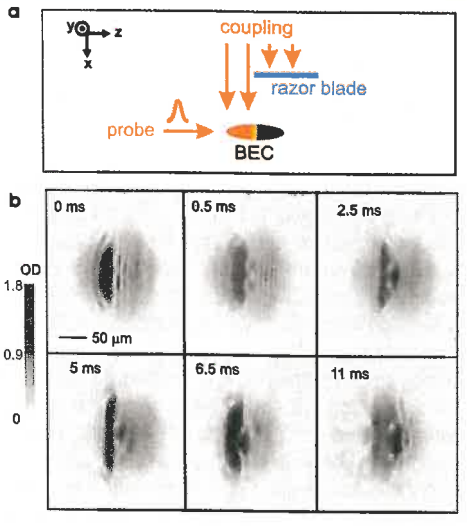

Fig. 5: Light Roadblock and Quantum Shock Waves in Bose-Einstein Condensates
(a) Light roadblock. A razor blade blocks the coupling beam from illuminating the far (*z>0*) side of the condensate. When the slowed probe light pulse reaches the roadblock (at *z=0*), where the coupling intensity drops to zero, the light pulse is further slowed and dramatically compressed to only a few microns, creating a narrow imprint of $|2\rangle$ atoms in the condensate. This imprint is kicked out (as in Fig. 2) and leaves a condensate of state $|1\rangle$ atoms trapped in the magnet, with a narrow density depletion in the middle. The narrow defect results in the formation of two density dips that propagate at the sound speed towards the condensate boundaries. Due to the dramatic variation of atom density and local sound speed across the structures, the back parts of the dips will catch up to the central parts, and the back edges will steepen. This process would in a normal fluid lead to shock wave formation. Here, where we form the defects in a Bose-Einstein condensate, we create the superfluid analogues of shock waves, 'quantum shock waves', in the form of topological defects (for example, dark solitons).
(b) Observation of quantum shock waves at the light roadblock (from ref. 10). After the density defect is formed at the light roadblock, we leave the condensate of $|1\rangle$ atoms trapped in the magnet for a varying amount of time (as indicated in the figures). We then abruptly turn the trap off and let the cloud expand for 15 ms. We subsequently image the central slice of the dropping condensate with the imaging beam (Fig. 1a) (the vertical height (along *y*) of the slice is 30 μm). We immediately observe (at 0 ms) the appearance of a series of white stripes (white means no condensate density), which indicate that dark solitons have been formed. The solitons are unstable, and the fronts are observed to curve after just 0.5 ms ('snake instability' [31]). The points along the main front, with large curvature, act as nucleation sites for quantized vortices, and at 2.5 ms we observe that two vortices have formed (seen as white dots in the figure). These two vortices are very stable, and they are clearly seen at 11 ms, for example. In the process, the overall shape of the condensate is also changing dramatically (indicating the presence of a large collective excitation of the condensate). At 5 ms the condensate is long, dense, and narrow. The condensate subsequently relaxes into the extended shape seen at 11 ms.

momenta could be of great importance for atom-interferometry.

Ultra-slow light also allows for extreme optics. Nonlinear optical effects associated with slow light are so large [1,29]—due to the steep refractive index profile—that nonlinear optics close to the single photon level is possible with micron-sized structures. For example, ultra-sensitive switches, with a switching energy corresponding to just two photons (10^{-18} Joule), and frequency up-conversion at very low power levels are possible.

With use of the light roadblock, light pulses have been compressed to sizes comparable to the wavelength of light, a very interesting regime for further studies. Furthermore, creation of vortices at the light roadblock makes possible unprecedented and direct studies of vortex collision dynamics in superfluids. Superfluidity is a property which allows BECs to flow without dissipation, and equivalently, superconductors to conduct currents with no resistance. Vortex collisions are expected to form the main mechanism by which dissipation is introduced into superfluid systems and are therefore of fundamental importance for understanding the breakdown of superfluidity and superconductivity.

Acknowledgement

The research was supported by the U.S. Airforce Office of Scientific Research, the U.S. Army Research Office OSD Multidisciplinary University Research Initiative Program, The National Science Foundation, and the National Aeronautics and Space Administration. CS was supported by a National Defense Science and Engineering Fellowship sponsored by the U.S. Department of Defense.

About the author

Lene Vestergaard Hau is Gordon McKay Professor of Applied Physics and Professor of Physics at Harvard University. She received her Ph.D. from the University of Aarhus, Denmark. She was named MacArthur Fellow in 2001 and just received the 2004 Richtmyer Memorial Lecture Award.

References

[1] Hau, L.V., Harris, S.E., Dutton, Z., and Behroozi, C.H., Light speed reduction to 17 metres per second in an ultracold atomic gas. *Nature* **397**, 594-598 (1999).

[2] Inguscio, M., Stringary, S., and Wieman, C., eds., Bose-Einstein Condensation in Aomtic Gases, *Proceedings of the International School of Physics Enrico Fermi, Course CXL*, (International Organisations Services, Amsterdam, 1999).

[3] Hau, L.V. Bose-Einstein condensation and light speeds of 38 miles/hour, in proceedings from the Workshop on Bose-Einstein Condensation and Degenerate Fermi Gases, Feb. 10-12, 1999 (Centre for Theoretical Atomic, Molecular, and Optical Physics, Boulder, CO) http://fermion.colorado.edu/~chg/Talks/Hau

[4] Liu, C., Dutton, Z., Behroozi, C.H., and Hau, L.V., Observation of coherent optical information storage in an atomic medium using halted light pulses. *Nature* **409**, 490-493 (2001).

[5] Kash, M.M., *et al.*, Ultraslow group velocity and enhanced nonlinear optical effects in a coherently driven hot atomic gas. *Phys. Rev. Lett.* **82**, 5229-5232 (1999).

[6] Budker, D., Kimball, D.F., Rochester, S.M., Yashchuk, V.V., Nonlinear magneto-optics and reduced group velocity of light in atomic vapour with slow ground state relaxation. *Phys. Rev. Lett.* **83**, 1767-1770 (1999).

[7] Phillips D.F., Fleischhauer, A., Mair, A., Walsworth, R.L., and Lukin, M.D., Storage of light in atomic vapour. *Phys. Rev. Lett.* **86**, 783-786 (2001).

[8] Turukhin, A.V., *et al.*, Observation of ultraslow and stored light pulses in a solid. *Phys. Rev. Lett.* **88**, 023602 (2002).

[9] Bigelow, M.S., Lepeshkin, N.N., and Boyd, R.W., Observation of Ultraslow Light Propagation in a Ruby Crystal at Room Temperature. *Phys. Rev. Lett.* 90, 113903-1 (2003).

[10] Dutton, Z., Budde, M., Slowe, C., and Hau, L.V., Observation of quantum shock waves created with ultra-compressed slow light pulses in a Bose-Einstein Condensate. *Science* **293**, 663-668 (2001).

[11] Harris, S.E., Electromagnetically induced transparency. *Physics Today* **50**, 36-42 (1997).

[12] Dalfovo , F., Giorgini, G., Pitaevskii , L.P., and Stringari , S., Theory of Bose-Einstein condensation in trapped gases. *Rev. Mod. Phys.* **71**, 463–512 (1999).

[13] Gustavson, T. L., Landragin, A., Kasevich, M. A., Rotation sensing with a dual atom-interferometer Sagnac gyroscope. *Classical Quant. Grav.* **17**, 2385-2398 (2000).

[14] Snadden, M. J., McGuirk, J. M., Bouyer, P., Haritos, K. G., Kasevich, M. A., Measurement of the earth's gravity gradient with an atom interferometer-based gravity gradiometer. Phys. Rev. Lett. **81**, 971-974 (1998); Peters, A., Chung, K. Y., Chu, S., Measurement of gravitational acceleration by dropping atoms. *Nature* **400**, 849-852 (1999).

[15] Dutton, Z. and Hau, L.V., in preparation.

[16] Dutton, Z., Ph.D. Thesis, (Harvard University, 2002).

[17] Burger, S., Bongs, K., Dettmer, S., Ertmer, W., and Sengstock, K., Dark Solitons in Bose-Einstein Condensates. *Phys. Rev. Lett.* **83**, 5198–5201 (1999).

[18] Manakov, S.V., On the theory of two-dimensional stationary self-focusing of electromagnetic waves. Soviet Phys. *JETP* **38**, 248-253 (1974).

[19] Busch, T., Anglin, J.R., Dark-bright solitons in inhomogeneous Bose-Einstein condensates. *Phys Rev. Lett.* **87**, 010401 (2001).

[20] Inouye, S., *et al.*, Observation of Feshbach resonances in a Bose-Einstein condensate. *Nature* **392**,151-154 (1998).

[21] Cornish, S.L., Claussen, N.R., Roberts, J.L., Cornell, E.A., and Wieman, C.E., Stable Rb-85 Bose-Einstein condensates with widely tunable interactions. *Phys. Rev. Lett.* **85**, 1795-1798 (2000).

[22] M. Kitagawa and M. Ueda, Squeezed spin states. *Phys. Rev. A* **47**, 5138–5143 (1993).

[23] Sorensen, A., Duan, L.-M., Cirac, J.I., and Zoller, P., Many-particle entanglement with Bose-Einstein condensates. *Nature* **409**, 63-66 (2001).

[24] Lukin, M.D., Yelin, S.F., and Fleischhauer, M., Entanglement of atomic ensembles by trapping correlated photon states. *Phys. Rev. Lett.* **84**, 4232-3235 (2000).

[25] DiVincenzo, D.P., The physical implementation of quantum computation, *Fortsch. Phys.* **48**, 771-783 (2000).

[26] Donnelly, R.J., *Quantized vortices in Helium II*, (Cambridge Univ. Press, Cambridge, 1991).

[27] Leonhardt, U., A laboratory analogue of the event horizon using slow light in an atomic medium, *Nature* **415**, 406 (2002).

[28] Bajcsy, M., Zibrov, A. S., Lukin, M. D., Stationary pulses of light in an atomic medium, *Nature* **426**, 638 (2003).

[29] Harris, S.E. and Hau, L.V., Nonlinear optics at low light levels, *Phys. Rev. Lett.*, **82**, 4611 (1999).

[30] Myatt, C.J., Burt, E.A., Ghrist, R.W., Cornell, E.A., and Wieman, C.E., Production of Two Overlapping Bose-Einstein Condensates by Sympathetic Cooling. *Phys. Rev. Lett.* **78**, 586-589 (1997).

[31] Anderson, B.P., *et al.*, Watching dark solitons decay into vortex rings in a Bose-Einstein condensate. *Phys. Rev. Lett.* **86**, 2926-2929 (2001).

Laser spectroscopy of nanometric gas cells

Martial Ducloy
Laboratoire de Physique des Lasers, Université Paris Nord, Villetaneuse, France

The Doppler effect was predicted by Christian Doppler during his stay in Prague in 1842 [1]. This effect is related to the propagation of oscillating waves (*e.g.*, sound waves, or light waves) and predicts the change of frequency of a wave emitted by a source, which is not static and moves either in the direction of the observer, or away from it : when the source approaches the observer, there is an increase in the frequency of the wave detected by the observer ("*blue shift*"), and when the source recedes, there is a decrease in the frequency ("*red shift*").

The Doppler effect plays an important role in the optical spectra of atomic or molecular species, from which one can analyse their characteristic emission frequencies. When these elements are in the gas phase (vapours, discharges, etc.), they are moving at random velocities, the distribution of which is centred at an average velocity u governed by the gas temperature (indeed proportional to its square root). This distribution of velocities induces a frequency broadening of the atomic emission lines (thermal or "Doppler" line-width), proportional to $\nu_{at}\, u/c$ (ν_{at}, atomic frequency; c, light velocity). The emission frequencies, which are essential for our understanding of the internal dynamics of atoms or molecules, and of their fundamental properties, cannot be measured with an accuracy better than the Doppler broadening.

The laser era, starting in 1960, revolutionised the field of optical spectroscopy. With the advent of laser sources, which are sources of monochromatic optical light that have a very high spectral purity (*e.g.*, their oscillation frequency ν has an extremely precise definition—in some cases, better than 10^{15}), and a very large brilliance or intensity, optical absorption spectroscopy took on a great importance. In particular, non-linear absorption spectroscopy became a very useful tool [2].

Among these methods, saturated absorption spectroscopy appeared as a method of paramount importance to get rid of the Doppler broadening of spectral lines. It makes use of the non-linear response of a resonant atomic or molecular gas to the irradiation by two counter-propagating laser waves of the same frequency ν_0. One wave excites the atomic species for a given velocity v_z, determined by the resonance condition $\nu = \nu_{at}$, where ν is the light frequency, taking into account the Doppler shift, $\nu = \nu_0(1\text{-}v_z/c)$. Because the other wave is counter-propagating to the first one, it probes atoms with opposite velocity, $-v_z$. Therefore, only for $v_z = 0$, the first wave will modify the propagation characteristics (absorption, dispersion, etc.) of the opposite wave, because of their simultaneous interaction with the same group of atoms having a zero velocity component along the propagation axis. This happens only for a laser exactly tuned to the atomic frequency $\nu_0 = \nu_{at}$, and allows for the elimination of the Doppler broadening, because of the velocity selection by a monochromatic laser source [2].

▲ **Fig. 1:** Photograph of "pill-box" cells. The interferometric modulation (fringes) of light reflected from the input cell of the window can be seen on the pictures. Each fringe corresponds to a thickness change of $\lambda/2$. The coin of 2 Euros (diameter 25mm) gives the scale of the figure.

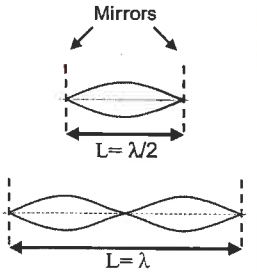

◀ **Fig. 2:** Vibration mode of a string fixed in two points at a distance L. The string oscillation is maximum ("resonance") for $L = \lambda/2$ (fundamental note, one spatial maximum), $L = \lambda$ (harmonics 2, two spatial maximums), $L = 3\lambda/2$, etc. An electromagnetic field propagating back and forth between two parallel mirrors (dotted lines) facing each other, reproduces the same type of resonant behaviour, because of the cancellation of the electric field at the mirrors' position.

An original approach, which has been pioneered by the late Venyamin Chebotaev of the Institute of Laser Physics, relies on the simultaneous absorption of quanta of light ("photons") coming from laser beams propagating in well-defined directions inside the atomic gas. In particular, if the atom absorbs simultaneously two photons of the same frequency, each travelling in counter-propagating directions, the Doppler shifts respectively associated with either absorption are exactly opposite, and their sum cancels, leading to a zero Doppler shift, whatever the atomic velocity may be [3]. This powerful technique, called "Doppler-free two-photon absorption" has been successfully applied to the spectral analysis of many atomic or molecular species.

More recently, another approach, developed in the 1980's, has relied on stopping and trapping atoms by using the radiation pressure induced on atoms by resonantly absorbed light [4]. When one photon is absorbed by an atom, this atom undergoes a kick ("photon recoil") in the direction opposite to the propagation direction of the photon. Atoms absorbing a photon propagating in a direction opposite to their motion are then slightly decelerated because of this recoil kick. They are finally stopped when they have absorbed enough photons. This is the very rapidly developing field of control of atomic motion by laser light [4]. For these stationary atoms, the Doppler shift is cancelled.

In the following a different approach is presented which makes use of ultra thin cells of atomic gas as laser light absorbers.

Gas dynamics and light absorption in ultra thin gas cells

"Ultra thin cells" are gas cells in which one dimension of the cell is much smaller than the other ones. They can be called "pill-box" cells [5]. Examples of such cells are given in Fig. 1. We have used such cells with thickness, L, which can vary from 10-20 μm, for the most common ones, down to 1μm or even 100nm, for the most recent ones [6]. The cell transverse dimensions are of the order of 2cm. The thinnest cells present an aspect ratio of 200000: to give an idea, this would correspond to digging a 60metre-wide hole, throughout the earth, between the two poles, or equivalently, to a

corridor, of width 1.8 km, linking the earth to the moon. The fabrication of these cells needs a special technology that has been described elsewhere (see Ref. [6]).

An important point is to know the cell thickness L accurately. To measure it, one makes use of the fact that the windows of the cell are partially reflecting the light (Fig.1). Thanks to the presence of two—input/output—windows, light reflection on the pill-box cell exhibits an interferometric behaviour as a function of the cell thickness. This is the so-called "Fabry-Pérot" effect that is related to the oscillating wave properties of light. One can understand it by analogy with the vibrations of a fiddle string: the oscillation amplitude of the string is enhanced when its length is equal to half of the oscillation wavelength (fundamental note) or to a multiple of this half wavelength ("harmonics") (Fig.2). These resonances correspond to a zero motion of the two extremities of the string which are fixed on a support. Similarly, a set of two parallel mirrors behave like a resonator for light—the "Fabry-Pérot" resonator: analogous resonances appear in the amplitude of light oscillating between the two mirrors (at the mirror position, the electric field must cancel). When the mirror spacing is a multiple of half the light wavelength λ, the transmission of incident light is a maximum, at the same time that its reflection is a minimum. The same behaviour applies to light reflection on a "pill-box" cell, with reflection minima occurring each time its thickness L is equal to n times $\lambda/2$. By monitoring light reflection for several wavelengths, one can then determine L with a very good accuracy (better than 4nm) in each point of the cell.

What is the dynamics of atoms inside this very peculiar type of "pillbox" cell? As an example, one can consider Caesium (Cs) atoms at room temperature: their mean thermal velocity is 200m/s. Then for a 1µm-thick cell, an atom flies, from one wall to the other, in an average time t = 5ns. By comparison the residence time of Cs atoms on a silica wall ("adsorption" time) is on the order of 5µs : there are one thousand more atoms adsorbed on the walls than freely-moving atoms in the gas!

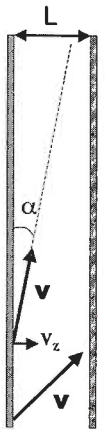

▶ Fig. 3: Geometry of the "pill-box" cell. An atom leaving the wall at a grazing incidence experiences a much longer time-of-flight.

A second noteworthy property of the gas dynamics is the fact that the time of flight of an atom between the two walls is highly anisotropic (Fig.3). An atom moving normal to the surfaces has an average "lifetime" of about 5ns, while an atom leaving the surface at grazing incidence has a much longer time of flight. For example, for a grazing angle α of one degree between the atom's velocity and the plane of the surfaces, the time of flight increases to about 0.3µs. The dramatic consequence is that the atoms that are moving nearly parallel to the surface interact for a much longer time with the light, and thereby contribute dominantly to the light absorption. When the incident light is normal to the surface, the Doppler effect cancels for those atoms moving at grazing incidence: the light absorption becomes free of Doppler broadening, as has been demonstrated in thin cells of Cs gas at the D_2 resonance line, λ = 852nm (Fig.4 , from Ref. [7]).

Singular properties of light transmission in ultra thin gas cells

The absorption spectrum shown in Fig. 4 has been recorded on a gas cell of thickness L = 10µm. When L is decreased to reach values of the order of the wavelength λ, novel coherent effects appear.

Fabry-Pérot effects

First, because of the "Fabry-Pérot" character of the two highly parallel windows (see previous section and Fig.2), the light amplitude is spatially modulated inside the cell, with intensity maxima when $L = n\lambda/2$ (n, integer). This intensity modulation strongly alters the overall amplitude of absorption spectra when L is varied, as well as that of reflection spectra [8].

Coherent character of the transient atomic response

The response of atoms to laser light excitation is essentially a transient one. Indeed the atoms adsorbed on one of the walls are perturbed in such a dramatic way that they cannot interact with the light. They are in equilibrium, *i.e.*, when they leave the wall, their internal energy is minimum and they are in the "*ground state*". Then, as soon as an atom quits the surface, it starts interacting with the resonant incident laser light and enters a transient absorption process. This transient response, which lasts for the whole time-of-flight of the atom in the case of ultra thin cells, is characterised by an oscillation of the atom's electronic charges (electric

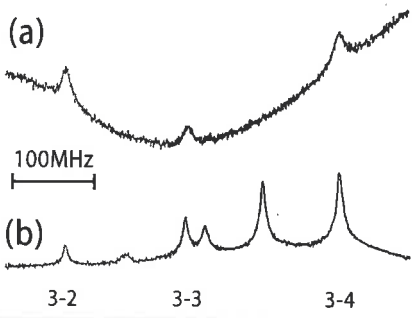

▲ Fig. 4: (a) Light transmission spectrum of a 10 µm-thick Cs cell, monitored near the Cs D_2 resonance line at λ = 852nm. The narrow spectral components are characteristic of the cell geometry and free of Doppler effect. They are revealing the atomic hyperfine structure of Cs. (b) Reference spectrum obtained by "saturated absorption" in a large cell (from Ref. [7]).

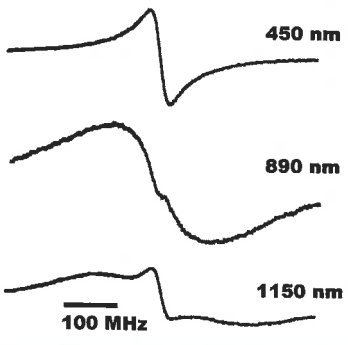

▶ Fig. 5: Light transmission spectrum observed at the Cs D_1 resonance line (λ = 894nm), in the "frequency modulation" mode (*i.e.*, the incident laser beam is frequency-modulated; FM), for various thickness of the Cs vapour cell. For $L = \lambda/2$, the spectral line is free of Doppler effect; at $L = \lambda$, the narrow line vanishes, and only remains as a wide Doppler-broadened component; for $L = 3\lambda/2$ (which is not exactly reached in the experiment, due to geometrical constraints), the narrow component does reappear, superimposed onto a Doppler-broadened background (from Ref. [11]).

dipole moment of the atom) driven by the oscillating electric field of the light. The phase of oscillation of the atomic dipole moment depends on its position in the cell. Summing up the various atomic dipole contributions to light absorption depends on their relative phase and leads to constructive or destructive interference, according to the cell length [9,10]. One has predicted and experimentally observed (Fig. 5) that the "Doppler-free" absorption resonance reaches a maximum amplitude for $L = \lambda/2, 3\lambda/2$, etc., and cancels for $L = \lambda, 2\lambda \ldots$ [11]. This length dependence is a clear signature of the coherent character of light absorption in ultra thin gas cells.

Wall attraction exerted on atoms

For still thinner cells ($L < 200$nm), the atoms start to feel the presence of the cell walls, even when they are moving at the centre of the cell. There is an attractive force between the atom and the surfaces. The electronic charges of the atom polarise the wall, inducing fictitious charges of opposite sign (the "image" charges) inside it. The resulting attraction between the atom's electronic cloud and its image appears at intermediate distances, $d \cong 10$-100nm; this is the so-called long-range, "van der Waals," or "London – van der Waals," atom-surface interaction [12].

Such a surface interaction acts on the atom as an external attractive potential, which lowers its internal energy. This attraction also shifts the resonance lines of atoms located close to a surface [13], because its strength depends on the atom internal state: for excited states of the atom, the electronic cloud is larger than for the ground state, implying larger charge fluctuations and larger surface attraction. Then, since the excited state energy is lowered more than that of the ground state, the atomic resonance frequency becomes smaller: this is the wall-induced "*red shift*" of the atomic resonance, which increases with decreasing atom-surface distances. This red shift has been observed in the transmission spectra of ultra-thin gas cells (Fig.6), and its thickness dependence (increased frequency shift with decreasing thickness) has been checked [14]. This is direct evidence of the ubiquitous van der Waals forces between neutral polarisable systems (here, an atom and a surface) which are of paramount importance in many fields of science and technology: physics, chemistry, biology, nanotechnologies...

Conclusion

Spectroscopy of microscopic (nanoscopic) gas cells gives access to a new regime of gas dynamics in which the thermodynamical equilibrium bscomes cell-specific. The corresponding atom-light interaction exhibits peculiar features, including a fully transient and coherent response, a strongly anisotropic atom time-of-flight and an explored space smaller than the wavelength. Transmission spectroscopy of ultra-thin gas cells allows one to study the field of Quantum Electrodynamics inside a dielectric nanocavity (where light is confined in a sub-wavelength space), as well as nanophysics and nanotechnology with "quasi interaction-free" atoms. It offers a way to explore long-range atom-surface interactions in a range of distances (~10nm) which has not been studied before. It should also give access to the peculiar characteristics of atom-atom interactions in a strongly confined environment. Further prospects include the engineering of the dielectric windows, in order to make them repulsive for a specific atomic state and the realisation of a novel type of material trap to prevent the atoms approaching the walls. To conclude let us quote as another field of application, frequency metrology. A laser, the frequency of which is stabilised on a perfectly defined atomic or molecular spectral line, provides an absolute frequency reference, *i.e.* an "optical clock". Ultra thin cells, with their opportunity for Doppler-free, linear spectroscopy in a tightly confined environment, are potential candidates for relatively compact, portable optical clocks.

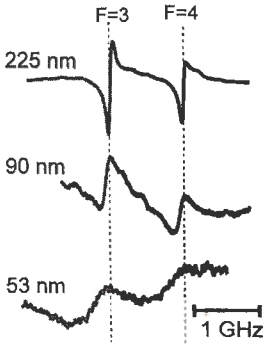

◀ **Fig. 6:** Wall-induced "red shift" of the Cs D_1 resonance line at $\lambda = 894$nm, as monitored on FM transmission spectroscopy for decreasing cell thickness ($L = 225, 90$ and 53nm).

Acknowledgments

This article is adapted from a presentation given at the general assembly of the Russian Academy of Sciences (RAS, Siberian Section, Novosibirsk) when the author received the honorary degree of foreign member of the RAS. The experiments presented here have been performed in "Laboratoire de Physique des Lasers" (LPL, Université Paris Nord), in collaboration with the Institute for Physical Research (IPR, Ashtarak, Armenia), where some of the technology of ultra thin cells has been developed. The author would like to thank Daniel Bloch, Stephan Briaudeau, Gabriel Dutier, Michèle Fichet and Marie-Pascale Gorza (LPL), David Sarkysian and Aram Papoyan (IPR), Alexander Yarovitski (Lebedev Physical Institute, Moscow) and Solomon Saltiel (Sofia University, Bulgaria) for their major contributions to this work.

About the author

Martial Ducloy graduated from Ecole Normale Supérieure and got his "Doctorat d'Etat" from Paris University in 1973. He is presently "Directeur de Recherche" CNRS, at Université Paris 13 (Villetaneuse), where he has been head of the Laser Physics Laboratory, Vice-President for Research (1986-93) and Dean for International Relations (1996-2002). He is Past-President of the EPS, and former chair of the EPS Quantum Electronics and Optics Division.

References

[1] See , *e.g.*, Christian Doppler's biography in *"EPS Biographies of European Physicists"*, Vol.1 (European Physical Society, Mulhouse, France, 2003)

[2] See, *e.g.*, V. S. Letokhov and V. P. Chebotaev, "*Nonlinear Laser Spectroscopy*" (Springer Verlag, Berlin, 1977)

[3] L. S. Vasilenko, V. P. Chebotaev and A. V. Shishaev, Pis'ma Zh. Eksp. Teor. Fiz. **12**, 161 (1970) [JETP Letters **12**, 113 (1970)]; B. Cagnac, G. Grynberg and F. Biraben, J. Physique (Paris) **34**, 845 (1973)

[4] S. Chu, C. Cohen-Tannoudji and W. D. Phillips, *1997 Nobel Lectures*, Reviews of Modern Physics **70**, 685-741 (1998)

[5] R.H. Romer and R.H. Dicke, Physical Review **99**, 532 (1955)

[6] D. Sarkisyan *et al.*, Optics Comm. **200**, 201 (2001)

[7] S. Briaudeau, D. Bloch and M. Ducloy, Europhysics Letters **35**, 337 (1996)

[8] G. Dutier *et al.*, Journal of the Optical Society of America **B 20**, 793 (2003)

[9] B. Zambon and G. Nienhuis, Optics Comm. **143**, 308 (1997)

[10] S. Briaudeau *et al.*, Physical Review **A 57**, R3169 (1998)

[11] G. Dutier *et al.*, Europhysics Letters **63**, 35 (2003)

[12] J.E. Lennard-Jones, Transactions of the Faraday Society **28**, 334 (1932)

[13] M. Oria *et al.*, Europhysics Letters **14**, 527 (1991)

[14] G. Dutier *et al.*, Journal de Physique **IV** (France) **12**, *Pr5*-155 (2002)

A new and exciting optically induced electron source: Extreme acceleration gradients beyond 1 TV/m

Victor Malka
Laboratoire d'Optique Appliquée (LOA)
ENSTA— Ecole Polytechnique— CNRS, France

Even today short-pulse, high-power and high repetition rate laser performances do permit the generation of electron bunches with new and interesting properties—particularly as they are routinely accelerated with gradients beyond 1 TV/m. These ultra short electron bunches were demonstrated to be well collimated (within a few degrees), energetic (up to 200 MeV) and bright (few nC). Since the same lasers system can additionally produce energetic proton bunches, such optically induced particle bunches appear to have interesting characteristics, which might enable a broad variety of applications ranging from nuclear, solid state and accelerators physics, through chemistry to Medicine.

In conventional accelerators such as LINAC's, acceleration gradients are limited to some tens of MeV/m due to material break down considerations. Consequently, as the energy gain of particles is the product of such gradients times the acceleration distance one is obliged to extend the acceleration distances in order to reach high energies. This is why these tools for current quests in high energy physics are becoming larger, and, even more importantly, more expensive. In contrast, a plasma is an ionised medium consisting of free electrons and ions, which thus cannot break down anymore. Therefore a plasma can support extreme electric fields and is likely to be a candidate for the next generation of particle accelerators, as was initially proposed by Tajima and Dawson [1]. Today huge gradients beyond 1 TV/m, i.e., more than 4 orders of magnitude greater than those produced with standard technology have been reported on [2]. Note closely, that these values are indeed the highest ever induced in a laboratory. As a consequence, with regard to the energy gain of particles in accelerators, this can cut down significantly the acceleration distance to boost particles from rest to several MeV over short distances—below the millimetre range and still provide high quality.

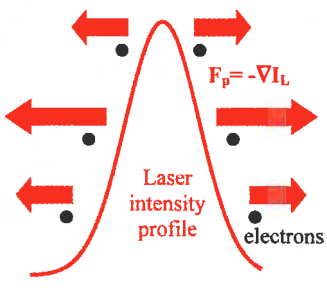

◀ Fig. 1: **Ponderomotive Force** This force expells electrons from regions of high laser intensity.

In order to understand the underlying laser plasma phenomena only a few parameters need to be defined in the following : the ponderomotive force, the plasma refractive index and finally the plasma wave with its associate electric field.

Ponderomotive force

As free electrons, such as are present in a plasma, can effectively quiver in the electric field of short-pulse lasers they are subjected to a variation of laser intensity. This can be expressed in the non-relativistic case with the fluid equation of motion within an electromagnetic field, which is also known as the Vlasov equation. This equation can be developed to second order to the ponderomotive laser force, which is a function of the laser intensity gradient. This ponderomotive force then, in particular present at the head of the laser pulse, pushes electrons ahead of the laser pulse—as is indicated in Fig. 1—in some kind of snow-plough effect. As a consequence, an electron plasma wave is created in its wake, which has a phase velocity equal to the laser group velocity, hence close to the speed of light. Note closely, as the ponderomotive force is proportional to the gradient of the laser intensity, this force is more dominant the shorter the laser pulse and the tighter its focussing.

Plasma index

The refraction index in a low density plasma with an electron density n_e is given by $n = 1 - n_e/2\gamma_\perp n_c$, where n_c is the critical density, which limits in general the laser propagation within a medium. The Lorentz factor $\gamma_\perp$ is given in the weakly relativistic regime by $\gamma_\perp = (1 + a_0^2/2)^{1/2}$, and it represents the relativistic mass correction of an electron oscillating in the laser electric field with a "laser vector potential," a_0, given by $a_0 = 0.86\,[I\,(\mathrm{W/cm^2})/10^{18}]^{1/2}\lambda(\mu\mathrm{m})$, where I is the laser intensity in (10^{18} W/cm^2).

Plasma wave and its associated electric field

A plasma wave is actually an electron density perturbation in space and time and its pulsation depends on the electron density, $\omega_p = (n_e e^2/\gamma_\perp m_0 \varepsilon_0)^{1/2}$. Such a plasma wave can easily be imagined by the oscillation of electrons around their initial nucleus. Due to this charge separation an electric field is induced, whose amplitude is given by $E = (m_e c\omega_p/e)\delta n/n$. An easy example shows that this can indeed yield tremendous values. Assuming a 1% electron density perturbation of a plasma with an initial density of 10^{17} cm^{-3} this corresponds to an electric field of 300 MV/m; and for a 100% density perturbation amplitude in a plasma at 10^{19}cm^{-3} the corresponding electric field even extends to 300 GV/m.

Producing electron bunches using only a laser beam

In order to realize this challenge a short-pulse laser with a power greater than a few TW has to be focused onto a gaseous target, typically a gas jet, since this can enable the laser to propagate through the medium. Assuming a laser peak intensity greater than 10^{18} W/cm^2, this gas jet is quasi-instantaneously ionised since the

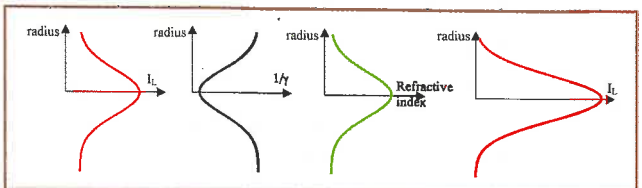

▲ Fig. 2: **Relativistic self focusing** The relativistic mass correction of electrons oscillating in the laser field can change the refraction index locally.

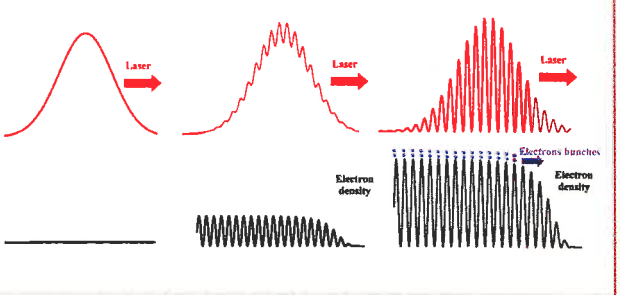

▲ Fig. 3: **The self modulated laser wake field scheme**
Here, the laser pulse length if much greater than the plasma wave wavelength.The initial Gaussian beam is modutated in a train of ultra short laser pulses whilst it is exicting a relativistic plasma waves. In case the amplitude of this plasma wave is high enough it can break and energetic electron bunches are generated.

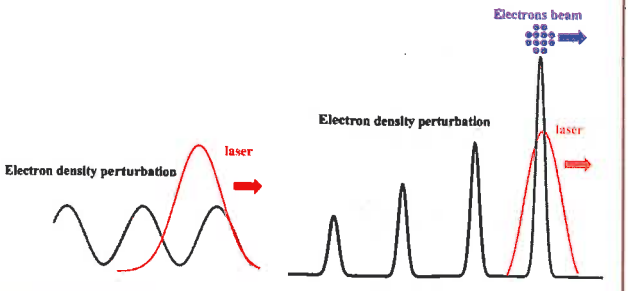

▲ Fig. 4: **Forced laser wakefield scheme**
Here, the laser pulse length is similar to the plasma wavelength. This plasma wave can reach the non-linear regime (very high amplitude plasma wave) producing record electric fields and a single bunch of energetic electrons.

corresponding laser electric field is much in excess of the atomic electric fields within the gas target. Consequently, the atomic Coulomb barrier is suppressed, electrons are liberated and a plasma is created. Since the laser can still propagate through this plasma as long as the plasma density is below the critical density, the interaction of the laser ponderomotive force and the free plasma electrons can drive a plasma wave, continuously increasing its amplitude. In the case that the amplitude of the plasma reaches a particular value dependent on the electron distribution temperature, this plasma wave breaks and plasma background electrons are trapped and boosted to high energy. In the following, two schemes will be discussed for this scenario: the Self-Modulated and the Forced Laser Wake Field regime.

a) The Self-Modulated Laser Wake Field Regime

Identified from numerical simulations in 1992 pursued almost simultaneously by three different groups [3], this regime was first shown to excite a high amplitude plasma wave. Here, a laser with a pulse duration in excess of the plasma period is required. Typically this means laser pulse durations greater than a few hundred fs. However, since high laser intensities are nevertheless needed for this experiment and the laser pulse length is somewhat long, huge laser energies are required, typically greater than a few tens of J.

Three years after this theoretical demonstration we have experimentally demonstrated this regime at Rutherford Appleton Laboratory (RAL) in the UK. In collaboration with English and American researchers from Imperial College and UCLA respectively, we have obtained an electron beam with a maximum energy of up to 44 MeV [4]. In this experiment the VULCAN laser was utilised, which delivered at that time an energy of 20 J per laser shot with a pulse duration of approximately 1 ps and a repetition rate of one laser shot every 20 min. Consequently, the laser power (in this case 20 TW) was greater than the critical laser power for relativistic laser self-focusing, $P_c(GW)=17\, n_c/n_e$. This relativistic laser self-focusing is due to the radial dependence of the plasma refractive index with laser intensity. As such, laser focal spots typically have a spatial Gaussian profile, the maximum velocity of electrons oscillating in the laser beam being higher the closer they are to the centre of the focus, where the laser intensity is the greatest. As the plasma pulsation is proportional to $(\gamma_L\, m_e)^{-1/2}$ the index of refraction of a plasma increases the faster these electrons oscillate. Graphically speaking, the plasma acts then as a focusing lens cancelling the natural light diffraction. This permits one to reach higher laser intensity over a distance longer than the Rayleigh length, i.e., than one could ever obtain in vacuum (see figure 2) [5]. Since in the Self Modulated Laser Wakefield regime the laser pulse length is in excess of the plasma wave wavelength, every fraction of the laser pulse "sees", due to this plasma wave, a different plasma electron density, and hence a locally different refractive index. Consequently, the laser pulse has locally different group velocities, which yields a bunching of the laser pulse envelope. This subsequently changes the laser ponderomotive force, which enhances the plasma wave amplitude. At the end a loop in between these two effects is induced, which can fully modulate the laser pulse envelop at the inverse of the plasma pulsation. This effect will grow in time and during the laser propagation in the plasma will transform the initial Gaussian laser shape into a train of shorter laser pulses with a duration proportional to $1/\omega_p$ (see figure 3). For this regime the generation of some 100 GV/m electric fields have been shown experimentally, which corresponded at the very end to an electron acceleration of up to 100 MeV.

b) The Forced Laser Wake Field Regime

As mentioned above, for these kinds of experiments high laser intensities are required. Since for the Self-Modulated Laser Wake Field regime a laser pulse length in excess of the plasma wave wavelength is needed, great laser energies are required. Another possibility to increase the laser intensity is naturally to shorten the laser pulse length, and hence the energy of the laser pulses can be less. However, the initial condition that the plasma wave wavelength is shorter than the laser pulse length might not be met anymore and the laser envelope cannot be modulated at the inverse of the plasma pulsation, even though the laser power is still beyond the

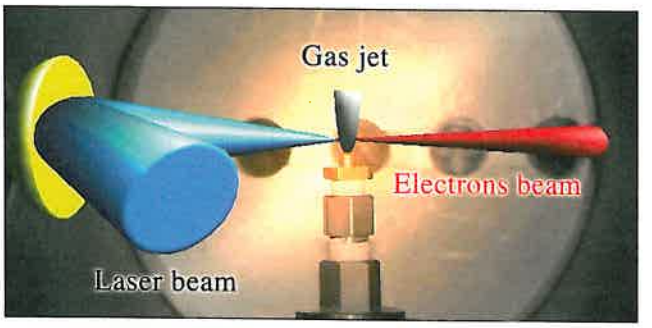

▲ Fig. 5: **Schematic of set-up**
The laser beam is the input and the electron beam the output.

laser critical power. Nevertheless, we have obtained a novel and indeed very promising acceleration regime where the laser pulse length is of the order of the plasma wave wavelength. This regime we call the Forced Laser Wake Field. The experiment validating this regime has been recently performed at Laboratoire d'Optique Appliquée (LOA/ENSTA/CNRS/Ecole Polytechnique) in France in collaboration with French researchers from CEA/DAM/DIF as well as CENBG and English researchers from Imperial College.

In the Forced Laser Wake Field regime [2] the laser pulse is short and intense, hence, the initial push due to the laser poderomotive force is so high that the laser pulses actually see a rising density ramp. Consequently, the head of the laser pulse is propagating in a region of high electron density, whilst the tail of the laser pulse is propagating in a density depression. Since in turn the laser group velocity at the tail of the laser pulse is higher than at its head, the tail catches up and the entire laser pulse is compressed by an optical shock (see Figure 4). Interestingly, this effect is dominant in a very localised space, i.e., in one plasma wave wavelength solely, which yields in turn extreme electric fields given by $E_{WB}\sqrt{2}(\gamma_p - 1)^{1/2} E_0$. Here, $E_0 = m_e c\omega_p/e$ is the electric field in the non-relativistic limit. Clearly, at an electron density of 2×10^{19} cm^{-3}, similar to the one defined in the experiment, the electric field reaches a record value of 1.4 TV/m.

The experiment

In contrast to the VULCAN laser mentioned above, the Ti:Sa laser in the "salle jaune" at LOA that was utilised in this experiment delivers 1 J, 30 fs laser pulses at a wavelength of 0.82 μm and at a repetition rate of 10 Hz [6]. The laser beam after compression propagates under vacuum conditions and is focused onto a gas jet (see figure 5). The gas jet profile has been optimised for this purpose (the cylindrical jet is homogeneous in density, additionally providing a sharp edge). The laser irradiance is, for the 1 meter off axis parabola, close to 3×10^{18}W/cm^2. Due to the high-quality front phase of these laser pulses a large fraction of about 50 % of this laser energy was concentrated in a small surface close to the diffraction limit of the laser. The electron density was controlled by changing the gas backing pressure of the jet. Here and as mentioned above the plasma pulsation (25 fs) was about the laser pulse duration (30 fs). A sketch of the experimental set-up is shown on Figure 6.

The electron beam produced in this experiment was characterized on the laser propagation axis both angularly and energetically with radiochromatic film and an electron spectrometer, respectively. The magnetic field of this electron spectrometer can be changed from 0 to 1.5 T, permitting one to decipher the electron energy in between 0 and 200 MeV with the help of silicon barrier diodes. A typical electron spectrum is shown in Figure 7, indicating a maximum electron energy of 200 MeV, twice as much as in the Self-Modulated Laser Wake Field regime and with a laser energy 20 times lower. This spectrum has a Maxwellian-like shape for electrons with energies below 130 MeV and shows a clear plateau for electrons with energies greater than 130 MeV. The Maxwellian component has an effective longitudinal temperature on the laser axis of 18 MeV. The angular distribution as shown in Figure 8 indicates that the higher the electron energy the better its collimation. The total charge of the entire electron pulse has in addition been measured and is close to 5 nC. Interestingly, and following the principles of standard classical accelerator physics, the normalized emittance of this electron pulse has been measured using the "pepper pot" technique. This has proven to be of a high quality, similar to that routinely produced at today's LINAC's where a normalized emittance of (2.7 ± 0.9) π mm mrad for electrons with an energy of (55 ± 2) MeV has been reported. The pulse length of this electron pulse has also been evaluated numerically in [7] and has been shown to be of the order of the of the laser pulse length, and hence in the sub ps range.

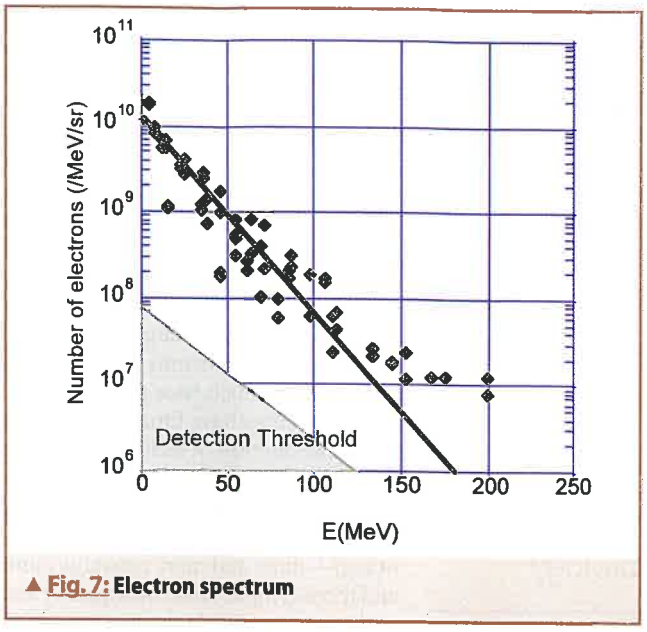

▲ Fig. 7: **Electron spectrum**

Conclusions and perpectives

In this article it has been shown how a high charge, energetic, low emittance and ultra-short electron beam can be produced with a compact laser system operating at 10 Hz. This electron source may permit very attractive applications in the near future in different domains such as material science, physics, chemistry,

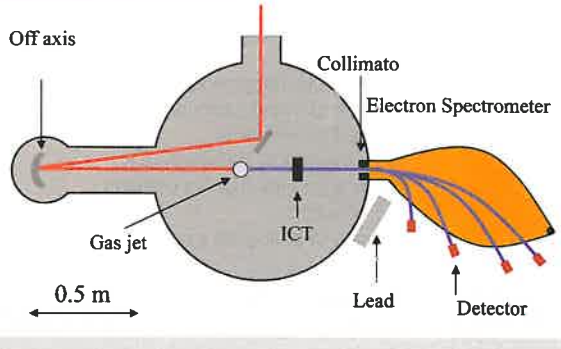

▲ Fig. 6: **Experimental set up**

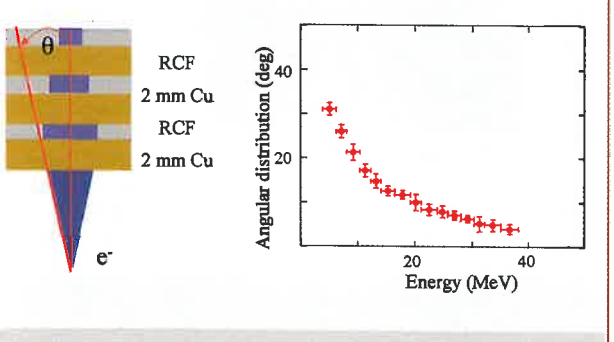

▲ Fig. 8: **Angular distribution**

accelerators physics as well as medicine. For example, irradiating a high Z target with this electron beam, a very small and energetic γ source could be generated. The perfect synchronisation of this electron beam with a laser beam might additionally permit new pump-probe experiments for example in ultra-fast chemistry [8].

This X-ray flash would permit time-resolved studies of fast phenomena in biology

An energetic X-ray source could be also produced by focusing the laser beam onto the electron beam. This X-ray flash would permit time-resolved studies of fast phenomena in biology within 30 fs accuracy [7]. Moreover the laser beam focused onto thin foil targets has already produced proton beams with energies up to 10 MeV. Such laser-generated proton beams may have future application in the production of radio-isotopes for PET [9], in proton therapy [10] and as a first stage of a proton accelerator. Indeed, the impressive progress seen in laser technology—more and more powerful, more and more compact and consequently less and less expensive laser systems—lead us and the entire laser plasma community to believe that this new approach to generating optically induced particle beams has the potential to change the scientific landscape in the near future.

Acknowledgements

The author acknowledges the help and support of the LOA teams, the Imperial College "plasma physic" group, Dr. E. Lefebvre and Dr. S. Fritzler for their expertise.

This article is based on an original version published in the Bulletin de la SFP" (French Physical Society), 140, p.20, July 2003.

About the author

Victor Malka, 43, is a CNRS permanent researcher at LOA (ENSTA, X, CNRS), senior scientist and lecturer at Ecole Polytechnique, Victor Malka is the head of the SPL group (Laser produced Particles Source).
Email: victor.malka@ensta.fr
SPL website: http://wwwy.ensta.fr/~loa/SPL/index.html

References

[1] T. Tajima, J. Dawson, *Phys. Rev. Lett.* **43**, 267 (1979).

[2] V. Malka *et al.*, Science, **298** (2002) 1596.

[3] N. E. Andreev *et al.*, JETP Letters **55**, 571 (1992), T. M. Antonsen and P. Mora, Phys. Rev. Lett. **69**, 2204 (1992), P. Sprangle *et al.*, Phys. Rev. Lett. **69**, 2200 (1992).

[4] A. Modena *et al.*, Nature **377**, 606 (1995).

[5] P. Monot *et al.*, Phys. Rev. Lett. **74**, 2953 (1995).

[6] M. Pittman *et al.*, Appl. Physics B, 74, 529 (2002).

[7] S. Fritzler *et al.*, Appl. Phys. Lett. **83**, 19 (2003).

[8] Y. Gauduel *et al.*, submitted to J. of Physics and Chemistry.

[9] S. Fritzler *et al.*, Appl. Phys. Lett. **83**, 15 (2003).

[10] C.-M. Ma *et al.*, *Med. Phys.* **28**, 1236 (2001), S. V. Bulanov and V. S. Khoroshkov, Plasma Phys. Rep. **28**, 5 (2002), V. Malka et al., submitted to *Med. Phys.*

The quest for brilliance: light sources from the third to the fourth generation

M. Altarelli[1] and Abdus Salam[2]
[1] *Sincrotrone Trieste, Area Science Park, Basovizza-Trieste, Italy*
[2] *International Centre for Theoretical Physics, Trieste, Italy*

It is evident that light is perhaps the most important tool by which we know the world around us. This is true not only for our everyday experience, but also for the scientific pursuit of an understanding of nature. Experiments using electromagnetic waves, in a range of wavelengths going well beyond the relatively small range of visible light, have played an important role in the development of modern science. Atomic and molecular spectroscopy, i.e. the study of the characteristic wavelengths emitted by matter in the gas phase, has been fundamental in establishing the laws of quantum mechanics and has given us important information on the composition of stars and planets. Einstein's brilliant 1905 interpretation of the photoelectric effect has opened the way to photoemission spectroscopy, which is still today one of the most important probes of the electronic structure of solids and solid surfaces, using UV light. Röntgen's discovery of x-rays in 1895, and the subsequent 1911 demonstration of x-ray diffraction by crystals, by von Laue and others, laid the foundations of crystallography, by which we can unravel the atomic structure of crystals. Every secondary school student is familiar with Watson and Crick's exploit of 1953 which identified the double helix structure of DNA from the x-ray diffraction work of Franklin and Wilkins, probably the most famous piece of crystallographic work ever.

It is therefore hardly surprising that scientists have been eager to obtain the brightest light sources, in order to understand the atomic and electronic structure of matter better and better. In parts of the infrared, in the visible and in the near UV, the invention of the laser has provided an extraordinary tool, which has led to many exciting discoveries and applications. Over a much broader range, encompassing not only the infrared and the visible, but also the whole of the UV and the x-rays to wavelengths well below 0.05 *nm*, the tool of choice for many scientists is synchrotron radiation (or *synchrotron light*) i.e. the bright emission of highly collimated electromagnetic waves from electrons (or positrons) orbiting at ultrarelativistic energies in storage rings with diameters of tens to several hundreds of meters (generally called with the slightly improper term *synchrotrons*). In spite of their large dimensions and associated cost, there are some 50 or so storage rings around the world built and operated solely for the purpose of producing light, and more are under construction.

Although synchrotron light is ever so popular today, the basic phenomena underlying this way of producing light are by no means very recent or novel. The electromagnetic theory of Maxwell, which very naturally contains aspects later formalised in the special theory of relativity, is all that is needed to predict the basics of synchrotron light. The radiation of accelerated charges, e.g of charged particles following a circular trajectory at constant speed, and subject therefore to centripetal acceleration, has a very different angular distribution depending on whether the speed of the particles is very small compared to the speed of light c (the classical limit), or very close to c (the ultrarelativistic case). In the latter situation, electromagnetic theory shows that the light emitted by the particles is confined to a narrow cone. The angular opening of the cone is given by $1/\gamma$, where $\gamma = E/mc^2$ is the ratio of the energy of the orbiting particle compared to its rest energy. Spectral analysis of the emitted radiation further shows that the emitted frequencies comprise all harmonics of the revolution frequency of the particle around the ring, from the fundamental up to harmonics of order $\sim \gamma^3$, above which the intensity drops rapidly. For an electron or positron of 1 GeV energy, γ is almost 2 000, whence the sub-*mrad* collimation of synchrotron light, and its broad spectrum, typical revolution frequency around large rings being in the *MHz* range, and $\gamma^3 \sim 10^{10}$–10^{12} for electron energies of a few GeV. In addition to these remarkable properties, synchrotron light also has well defined polarisation properties. To understand why the light is so bright one has to consider how large the acceleration is for a particle which is going at essentially the speed of light in one direction and that half a circumference (i.e. typically ~ 1 μs) later is moving at the same speed in the *opposite* direction!

The first description of the emisssion of relativistic particles following a circular orbit is given in 1912 by Schott, and received little attention. The problem became of high interest in the 1940's, when it became apparent that the main hurdle in the construction of higher and higher electron energy accelerators is the rapid growth of the radiated power with electron energy (proportional to E^4 for a fixed radius of the machine). The modern derivation of the basic expressions used in the description of synchrotron radiation was provided by Schwinger in the USA and by Ivanenko and Pomeranchuk in the Soviet Union. The first direct observation of synchrotron radiation was reported in 1947 by Elder *et al.* at the 70 MeV Synchrotron in the General Electric Laboratories in Schenectady, NY (USA) [1].

First, second and third generation light sources

The driving force behind the development of light sources is the optimization of their *brilliance* (or spectral brightness), which is the figure of merit of many experiments. Brilliance is defined as a function of frequency given by the number of photons emitted by the source in unit time in a unit solid angle, per unit surface of the source, and in a unit bandwidth of frequencies around the given one. The units in which it is usually expressed are *photons/s/mm²/mrad²/0.1%BW*, where *0.1%BW* denotes a band-

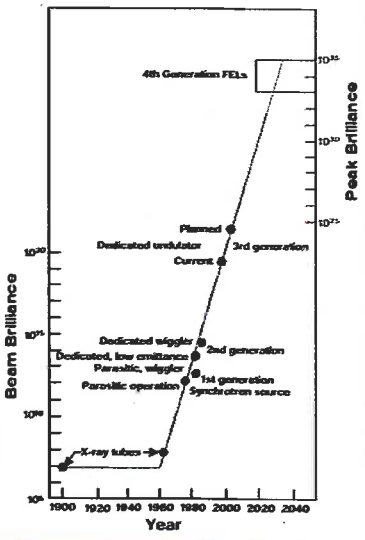

Fig. 1: (after D. Moncton) Historical evolution of the brilliance of 8 keV x-ray sources, extrapolated into the future. The left scale represents the average brilliance (averaged over the pulsed structure of the synchrotron beams), the right scale refers to the peak brilliance (at the top of one pulse).

features

▲ Fig. 2: View of Elettra, a third generation light source in Trieste.

width $10^{-3}\omega$ centered around the frequency ω. As one can appreciate from the definition, brilliance puts a premium not only on the photon flux (photons per second in a given bandwidth), but also on the high phase space density of the photons, i.e. on being radiated out of a small area and with high directional collimation. Liouville's theorem ensures that brilliance is a property of the source and not of the optics of the beamline which delivers the photons to the experimental station. An ideal set of optical elements can only preserve the brilliance, a real one will always degrade brilliance (as some photons get lost on the way down the beamline). The brilliance of available synchrotron sources has been growing at a formidable pace in the last decades (see Fig. 1), since the first attempts at a systematic exploitation of storage rings as sources of photons for scientific experiments in the 1960's.

At that time, some electron storage rings designed and built for nuclear and subnuclear physics started to be used *parasitically*, for some fraction of the time, as sources of photons for experiments in atomic, molecular and solid state physics. These machines are nowadays referred to as "first generation light sources". The experimental results were so interesting and promising to stimulate the construction of dedicated rings, designed and optimised to serve exclusively as light sources. Examples of these "second generation" machines are the BESSY I ring in Berlin, the two National Synchrotron Light Source rings in Brookhaven, NY (USA), the SuperACO ring in Orsay, near Paris, and the Photon Factory in Tsukuba (Japan). In the 1990's a new generation of rings started operation. These "third generation" synchrotron sources are characterized, as we shall briefly explain below, by a reduced emittance (i.e. reduced phase space volume) of the circulating particle beam, and by the extensive use of undulators as radiation sources, with a further increase of the brilliance by several orders of magnitude. Examples of this generation of sources are the European Synchrotron Radiation Facility (ESRF) in Grenoble, the Advanced Light Source in Berkeley, California, Elettra in Trieste (see Fig. 2), BESSY II in Berlin, Max-II in Lund, Sweden, the Advanced Photon Source, in Argonne, Illinois, Spring 8 in Japan, and the Swiss Light Source in Villigen (CH).

Two basic advances, as has been mentioned before, made the transition to the third generation possible. On the one hand, the progress in the design and fabrication of the lattice of magnets that guide the electrons (or positrons) around the storage ring allowed a reduction in the size of the cross section of the circulating particle beam, and a better collimation (parallelism of the velocities of all particles at a given point in the ring). This can be expressed quantitatively as the volume of the phase space projection along the horizontal plane of the particles' trajectory (horizontal emittance). This quantity is measured in *nm rad* (nanometers times radians). It is typically of order 30-100 *nm rad* or more in a second generation machine, and typically of order 5 *nm rad* in a third generation ring. It is intuitive that the properties of small beam cross section and high collimation of electrons translate into corresponding properties of the radiated photons and therefore contribute to the brilliance. The second advance is the development of insertion devices (wigglers, and most importantly undulators) which are arrays of magnets, typically 2 to 5 *m* long, inserted in a straight section of the ring, and which produce a vertical magnetic field with a sinusoidal dependence along the electron trajectory (see Fig. 3). The resulting Lorenz force on the drifting electrons modifies their straight trajectory into a zig-zag one, producing a large number of bends with intense radiation emission. Wigglers are large field devices, which produce deviations of the beam from the straight trajectory that are large when compared to the characteristic angle of synchrotron radiation emission, i.e. $1/\gamma$. The radiation cones from each bend of the trajectory do not overlap and the wiggler multiplies the number of bends, preserving the same broad spectrum of emitted wavelengths. The undulator, on the other hand, is a small field device, where the largest deviation of the electrons from the straight line is at most of order $1/\gamma$, so that radiation cones from the whole trajectory of an electron spatially overlap, and the resulting electromagnetic fields interfere. Detailed calculations show that the result of the interference is to enhance emission at a particular wavelength and at its harmonics and to suppress it elsewhere. These wavelengths are given by:

$$n\lambda = (\lambda_0 / 2\gamma^2)\,(1 + K^2/2),$$

where λ_0 is the period of the sinusoidal magnetic field of the device, $K = \gamma\theta$, θ being the electrons maximum angle of deviation from the straight trajectory, and $n = 1, 2, 3, \ldots$ is the order of the harmonic.

Interference phenomena in undulators, therefore, concentrate the brilliance around a discrete set of wavelengths. It is however very important to notice that the fundamental wavelength is tunable by the mechanical movement of the magnet arrays: when their distance varies, so does the maximum magnetic field and therefore the maximum deviation angle θ and the K parameter. Undulator radiation can be characterized as quasi-monochromatic and *tunable*.

There are about ten years of experience in the operation of third generation light sources. Examples of the breakthroughs which were made possible by these remarkable scientific instruments in a variety of fields, encompass condensed matter physics, materials science, chemistry, mineralogy, biology and even medical and industrial applications. Certainly more will follow in the years to come; nonetheless scientists have been wondering about the next step, i.e. the concepts necessary to bring about a further increase in brilliance by a few orders of magnitude.

Fourth generation light sources: Free Electron Lasers and recirculating machines

One feature of the storage ring as a light source is that the same electrons turn for hours and hours, going hundreds of thousands and even millions of time per second through the same undulators and dipole magnets. The radiofrequency cavities in the ring give back the radiated energy to the electrons (they typically radiate about 0.1% of their energy at each turn) so that they keep turning and turning. Every times an electron emits a photon, a non-deterministic quantum process, recoil effects perturb its

momentum and position. These millions and millions of "random" perturbations per second determine a lower limit to the emittance that the magnetic lattice of the ring can impose on the electrons, i.e. they prevent the phase space volume of the electrons from being too small. A careful and thorough quantitative analysis show that it is not possible to lower substantially the emittance of a storage ring below the values achieved in third generation machines. This is the reason why the pursuit for the fourth generation has oriented itself to "single-pass" or "few-passes" machines, where a given electron goes only very few times through an undulator.

One possibility is to abandon the ring geometry and consider a linear accelerator, or Linac, which feeds the accelerated electrons into a long undulator. At the end of a Linac, it is foreseeable - and to some extent already experimentally proven—that very low emittance and also very short electron bunches (~ 100 fs, as opposed to the ~ 50 ps typical for storage rings) can be produced. The generation of correspondingly short x-ray photon pulses was recently demonstrated in Stanford, in the SPPS project at the SLAC Linac, where bright ~ 80 fs x-ray pulses were generated by a standard undulator [2]. But a carefully designed and very long undulator at the end of a suitable Linac can produce radiation with full spatial coherence, i.e. laser-like and delivered in sub-ps pulses of extremely high peak brilliance (exceeding 10^{29} – 10^{30} *photons/s/mm²/mrad²/0.1%BW*, to be compared with ~ 10^{21} for third generation undulators). This is the extraordinary promise of Linac-based Free Electron Lasers (FEL's). The difference between "spontaneous" or "incoherent" undulator radiation and FEL radiation is that in an undulator, as was briefly explained, there is constructive interference between the fields radiated by one electron at different points of its trajectory. In the FEL process, the fields of *different* electrons also interfere constructively. This is possible if the distribution of electrons within the bunch is not uncorrelated, but there are density modulations with the wavelength of the undulator resonance. If the undulator is long enough and the bunch has suitable properties, these density fluctuations can be imprinted by the radiation itself. Consider indeed the progress of a bunch of electrons down the undulator. The light emitted at the back of the bunch goes a little bit faster than the electrons (the latter travel at a speed slightly lower than *c*, and have a wiggly trajectory due to the magnetic field, while photons go straight!). The light wave, therefore travels down the bunch and, interacting with the electrons, it imparts a density modulation at its wavelength. In point of fact, the process is helped by the spontaneous density fluctuations statistically arising inside the electron bunch: the travelling light wave enhances dramatically those of the corresponding wavelength. The modulated bunch radiation starts to grow exponentially down the undulator length, until saturation is reached. This mechanism is known as SASE, or Self-Amplified Spontaneous Emission and produces full spatial coherence for radiation of very short wavelength. This has been demonstrated at DESY in Hamburg for wavelengths down to 80 *nm* [3], using the superconducting Linac technology, and progress towards the goal of 6 *nm* is underway.

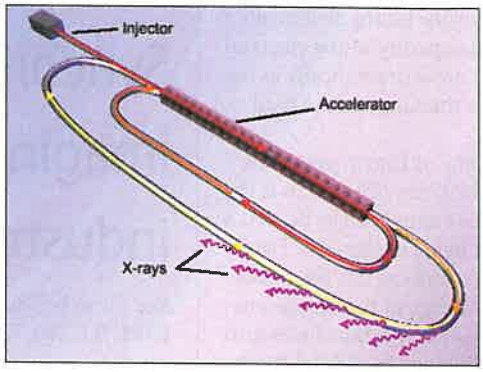

◀ **Fig. 4:** Scheme of principle of an energy-recovery Linac. Electrons from the injector are accelerated in the Linac, then recirculated in the Linac a first time via the first arc section to be accelerated to the final energy; at their maximum energy, electrons circulate in the larger arc section where they radiate into many beamlines, before returning to the Linac to give back most of their energy to the RF cavities.

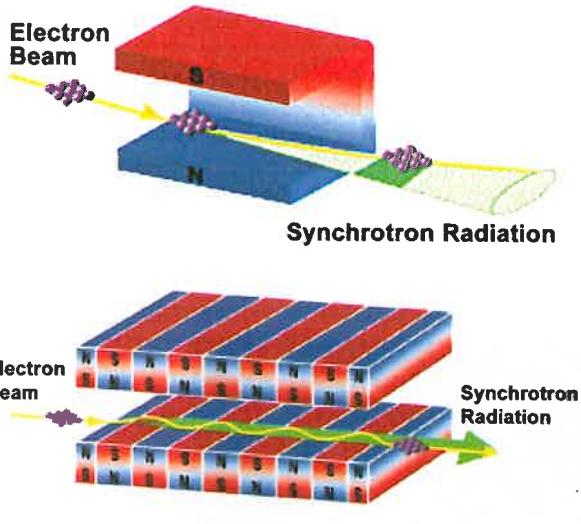

▲ **Fig. 3:** (Top) Schematic view of the generation of synchrotron radiation in a dipole bending magnet, where electron bunches are deviated to follow the orbit around the ring.
(Bottom) Generation of synchrotron radiation in an insertion device, where the upper and lower magnet arrays produce vertical fields forcing the electrons to follow a zig-zag trajectory.

The idea of pushing this project to 0.1 *nm* within a European X-ray FEL Laboratory, on the model of the ESRF, is presently being discussed. A similar project (the LCLS, "Linac Coherent Light Source") using the room-temperature SLAC technology is underway in Stanford.

There are also many smaller projects to generate VUV and soft x-ray coherent radiation, also based on linear accelerators, each of them with some specific feature that makes them quite complementary to one another. Some of these do not envisage reliance on statistical fluctuations to induce the initial density modulation in the electron bunch, but aim to induce it externally, with a pulsed laser synchronised to the electron bunches. It turns out in fact that an electron bunch in the magnetic field of the undulator behaves as a strongly non-linear optical medium. An external laser of wavelength λ can generate density modulations with components not only at λ but also at the harmonics λ/n, so that a visible or near UV conventional laser can generate modulations of much shorter wavelengths. The light of a first undulator could induce even shorter wavelength modulations in a second one, in a harmonic cascade process. The advantage of these "seeded" FEL schemes is the very precise control of the pulse timing, as the FEL pulses are triggered by the predictable pulses of the external laser, and not by the random noise of the density fluctuations in the electron bunch. An example of such a project is the FERMI@ELETTRA seeded FEL, with the ultimate goal of achieving 10 *nm*.

The scientific scenarios opened by 100 *fs* long, spatially coherent pulses of UV and x-radiation are very exciting. This explains the large number of projects that are being pursued or proposed at var-

features

ious laboratories around the world. Clearly the technical difficulties connected with the requirements on the quality of the electron bunches (emittance, peak current, etc.) grow dramatically as the required wavelength decreases towards the range of the hard x-rays.

In the pursuit of the higher brilliance of fourth generation sources there is an alternative road to the Linac FEL's . This is the approach based on recirculating Linacs, as exemplified by the 4GLS ("4th Generation Light Source") project being designed at Daresbury Laboratory in the UK. The idea is to combine the "few passes" strategy to lower emittance with the advantage of the ring geometry in which a large number of tangential beam lines and experimental stations can be exploited by users in parallel. It consists of a Linac that feeds electrons into one or several arc-shaped sections on which undulators, wigglers and even FEL's can be inserted (Fig. 4). At the end of the (last) arc, electrons are either dumped or fed back into the Linac, where they can return part of their energy to the RF fields in the accelerating cavities (this latter version is called "energy-recovery Linac"). The Linac is preferably of the superconducting type, one of the reasons being that it can support a much higher repetition rate (a much smaller time interval between successive bunches).

Conclusions

The interest of scientists from a variety of disciplines in ever more brilliant light sources in the UV and x-ray spectral region is not decreasing. While the third generation sources are still delivering a wealth of interesting science, the intense activity to generate spatially coherent, ultrashort pulses promises a new frontier to be opened a few years from now. It will be extremely interesting to monitor the progress of the many projects underway all over the world.

About the author

Massimo Altarelli was trained at the University of Rome as a condensed matter theorist. At the ESRF in Grenoble, he was Research Director (1987-1993), and Head of the Theory Group (1994-1998). Since 1999 he has been in Trieste on the staff of the International Centre for Theoretical Physics, and Director of the Elettra Synchrotron Light Source.

References

[1] An excellent account of the early history of synchrotron radiation, with many references, can be found on pages 27-35 of E.-E. Koch, D.E. Eastman and Y. Farge, "Synchrotron radiation – a powerful tool in science", in *Handbook of Synchrotron Radiation*, vol 1A, E.-E. Koch editor (North Holland, Amsterdam, 1983) pp 1-63;

and also at the site http://xdb.lbl.gov/Section2/Sec_2-2.html, which provides an account by A.L. Robinson, as part of the X-ray Data Booklet Project of Lawrence Berkeley National Laboratory.

[2] See http://www-ssrl.slac.stanford.edu/jhhome.html for a short description of the state of the project

[3] J. Rossbach, Nucl. Instr. Meth A475, 13 (2001); for a first experimental application, see H. Wabnitz *et al.*, Nature 420, 482(2002)

Synchrotron radiation imaging and diffraction for industrial applications

José Baruchel and Åke Kvick
ESRF, B.P. 220, 38043 Grenoble, France

The use of the modern synchrotron radiation (SR) sources for X-ray imaging and diffraction provides new possibilities for applied science and technology. They include an enhanced resolution (spatial and/or temporal), the possible use of the coherence of the beam, in-situ experiments and accurate quantitative measurements of local density or strain. Selected applications showing the improved capabilities in absorption or phase microtomography, time-resolved diffraction experiments showing the way a lithium-based battery works, or strain measurements on stir-welding materials, are presented as examples. The combination of diffraction and imaging (i.e. diffraction with micron spatial resolution) allows further applications, such as the study of grain growth, or the X-ray topographic investigation of defects responsible for spurious modes in single crystal resonators.

The aim of the present paper is to highlight the contribution of synchrotron radiation X-ray imaging and diffraction to the investigation of industrial topics. These techniques, which allow the visualization of the volume of systems opaque for other probes and the determination of their structure, have been dramatically renewed by the use of modern, "third generation", synchrotron radiation (SR) facilities beams. Real time/high-resolution experiments are performed for both X-ray imaging and diffraction. The high energy of the available beams allows the deformation within bulk materials to be investigated. The high coherence of the beam allows phase contrast imaging to be exploited, the contrast arising from phase variations across the transmitted beam. Absorption and phase microtomography provide three-dimensional information on features like cracks, porosities or inclusions, which are of high interest for applied topics such as metallurgy, polymers, or reservoir rocks containing fuel. The spatial resolution of these techniques is now in the 1 μm range. Lastly the combination of diffraction and imaging, through the new tracking techniques, or the use of Bragg diffraction imaging (X-ray topography) provides additional information on industrially interesting materials.

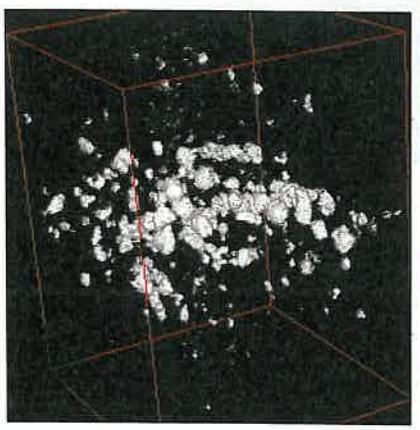

◀ **Fig. 1:** 3D image of the distribution of holes (in white) within a copper target (transparent), 269*284*201 pixels, 2 μm voxel size

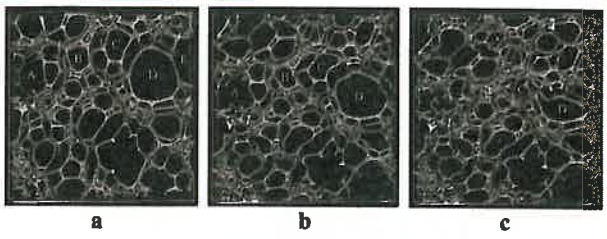

▲ Fig. 2: Reconstruction of an open-cell flexible polyurethane foam at several levels of compressive strain. (a) 0%, (b) 10%, (c) 23%, these percentages being the ratio of the variation of vertical length of the foam over the original, unstrained, length. The 3D renditions represent volumes of 7mm × 7mm × 1.4 mm.

The original features of third generation synchrotron radiation facilities such as the APS, ESRF, or Spring 8, for imaging and diffraction applications, are:

a) the very high intensity of the X-ray beam (factor 10^6 with respect to usual X-ray generators); both white and monochromatic beams can be used
b) the availability of photons spanning the whole range from the infrared to hard X-rays (up to 300-400 keV)
c) the design of beamlines optimised for a given set of techniques
d) the small size of the electron beam cross-section (< 100 μm), which leads to high brilliance, and to a sizeable lateral coherence of the X-ray beam.

Absorption and phase microtomography

The principle of microtomography is very similar to that of the well-known medical scanner. When applied to materials investigation, it consists in recording a series of radiographs (typically of the order of 1000) for different angular positions of the sample, which rotates around an axis perpendicular to the beam. Several laboratory microtomographs have been commercially produced over the last years (Rüegsegger *et al.*, 1996, Sasov and Van Dyck, 1998). But the best images, in terms of spatial resolution, signal-to-noise ratio and quantitative exploitation, are obtained using synchrotron radiation. This results from the high intensity, practically parallel and monochromatic incoming beam. In this approach there is no image magnification, and the spatial resolution mainly results from the effective pixel size of the detector. The range of pixel sizes available at the ESRF goes from 0.3 μm to 30 μm, and a big effort is being produced to enhance the spatial resolution down to the 100 nm range. The total acquisition time is in the 10^{-2} ("fast tomography") to1 hour range, and the recorded data is often several Gigabytes.

An increasing number of applied or industrial research laboratories require the use of microtomography to solve some of the problems they encounter. To achieve this requirement they either buy beamtime and expertise, or have access to the synchrotron facilities through collaboration with Universities or research groups and peer-reviewed proposals. The industrial requirements include, most of the time, confidentiality, rapid access and full service. Most facilities, and in particular the ESRF, propose such a service, going from the experiment to the data analysis (volume reconstruction, extraction of relevant parameters ...).

Figure 1 is an example of such application-oriented investigation. A strong impact on a copper target creates porosity within the bulk metal. The investigation of the pore sizes and distribution is of high importance for applications. The only way to image these pores inside such a sample is X-ray microtomography (Bontaz-Carion *et al.*, 2001). The spatial distribution of pores within one of these copper samples was determined (figure 1), and shown to be less homogeneous, both from the point of view of size and of location, than what was expected from theoretical models.

Another example of absorption tomography, which implies a specially designed sample environment cell, is the in-situ investigation of an open-cell polyurethane foam at several levels of compressive strain (figure 2). This work, performed by a research group from ICI Polyurethane in collaboration with a group of the University of Cambridge, correlates the macroscopic behaviour (stress/strain curve) with the local structure modifications. It shows that the initial phase of compression, which is associated with a linear elastic response, corresponds to a bending of the struts, whereas the plateau in the stress/strain curve is linked to the collapse a whole band of cells (Elliott *et al.*, 2002). This result was known from surface observations, but no volume evidence was available.

The X-ray beams produced at third generation synchrotron radiation facilities exhibit a high degree of coherence. This results from the small source size σ (in the 50 μm range) and the large source to sample distance L (in the 100 m range). The transverse coherence length $d_c = \lambda L/2\,\sigma$, is in the 100 μm range, and allows "phase images" to be recorded by just varying the sample-to-detector distance ("propagation technique", reviewed for instance by Cloetens *et al.*, 1999a). The great advantage of this new type of imaging is the increased sensitivity it provides, either for light materials such as polymers, or for composites made up of materials with neighbouring densities (for example Al and SiC). A first use of the phase images relies on the visualisation of the phase jumps that occur at the edges of a particle or porosity imbedded in a matrix having a different index of refraction. Phase microtomography based on the visualisation of the edges was used, for instance, to understand the mechanisms of degradation in Al-SiC composites. It was possible not only easily to visualize the SiC reinforcing particles, but also to observe the nucleation and propagation of cracks when the material is submitted, *in situ*, to tensile stress. The cracks appear first in the elongated particles, and their number is 50% more than suggested by surface investigations (Buffière *et al.* 1999).

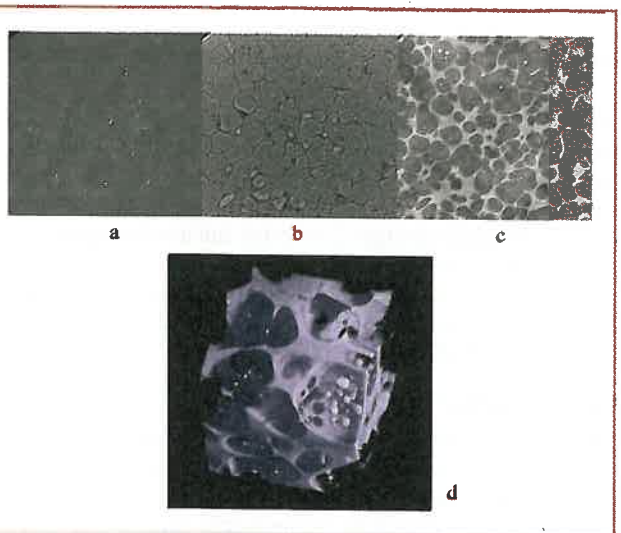

▲ Fig. 3: Tomographic images of an Al-Si alloy, quenched from the "semi-solid" state a) Detector to sample distance D = 0.7 cm b) D =60 cm c) "holotomographic" image, d) 3D rendering showing the former "liquid" phase (courtesy L. Salvo and P. Cloetens).

features

Phase imaging based on the detection of the edges does not allow the local phase to be extracted quantitatively, and its spatial resolution is limited by the occurrence of the fringes used to visualize the borders. A more quantitative approach of phase imaging and tomography was developed. It is based on the combination of several images recorded at different distances. An algorithm, initially developed for electron microscopy by the Antwerp group, was successfully adapted to the X-ray case, and allows the "holographic" reconstruction of the local phase, well beyond the images of edges (Cloetens *et al.*, 1999a). Once the phase maps are obtained through holographic reconstruction, there is no conceptual difficulty in bringing together many maps corresponding to different orientations of the sample, and in producing the tomographic, three-dimensional, reconstruction procedure. For each of the angular positions of the sample, the phase map is retrieved using images recorded at several (typically four) distances. The highest accessible spatial frequency is determined by the resolution of the detector. This combined quantitative phase mapping and tomography procedure, called **holotomography** (Cloetens *et al.*,1999b), provides a very useful approach to the characterization of materials on the micrometer scale.

The "holotomographic" procedure was applied to an Al-Si alloy, quenched from a temperature where a "mainly Al" solid phase is surrounded by an Al-Si liquid one. This is an important industrial material because in the "semi-solid" state it is possible to give a desired shape to the alloy, this shape being retained when cooled to room temperature. The density difference between the two phases is in the 1-2% range. For each angular position of the sample 4 images were recorded at different distances, yielding 3D quantitative images that show, with a voxel edge size of 1 μm, the distribution of electron density, hence of mass density, in the sample. The highest accessible spatial frequency is determined by the maximum resolution of the detector (~1-2 μm). Fig 3 compares the possibilities of absorption microtomography (fig. 3a, where the phases are indistinguishable, and only iron-rich metallic inclusions are visible) with edge-enhancement phase microtomography (fig. 3b, where the phase boundaries are outlined by a black-white line) and with holotomography (fig. 3c, where the two phases are clearly observable through their grey level), and shows in 3d) a 3D rendering of what was the "liquid" phase.

Diffraction experiments on industrially related topics

The accessibility of hard penetrating X rays that can be focussed into sub micron spots while retaining extremely high probe intensity has opened up the field of diffraction to industrially interesting fields. New experiments with millisecond time-resolution, sub micron spatial resolution with bulk probing capability of several tens of centimetres in high Z materials can now be performed to map out stress/strain fields, to follow reactions in real time or to study *in situ* processes in complex environments such as inside reaction vessels or even in working devices like batteries or other electrochemical cells.

Time resolution

Time-resolved studies tend to fall into three categories: the second to several minute processes, millisecond to microsecond processes and extremely fast pico-second reactions. The last category can only be studied at present by "stroboscopic" experiments were the process is repeated many times to obtain sufficient counting statistics. Most industrial reactions however fall into the first two categories and are usually irreversible ruling out stroboscopic measurements. The present synchrotron facilities provide sufficient x-ray flux to perform one-shot experiments well down in time to the microsecond regime. The 2 dimensional diffraction data is recorded by fast read-out detectors such as large CCD cameras.

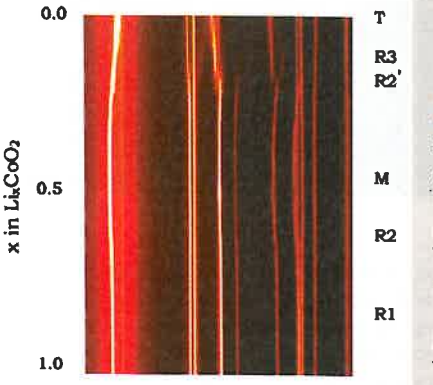

◀ **Fig. 4:** Diffraction patterns collected during *in situ* reduction of Li_xCoO_2 batteries. The letters on the right indicate the different structural phases through which the electrode material passes.

An example is given by the in-situ study of an electrochemical reaction experiment on a working Li_xCoO_2 battery (Morcrette *et al.* 2002). Strong diffraction spots from highly crystalline current collectors and packaging material have in the past compromised the weaker diffraction from the material under study. In order to de-emphasise the strong diffraction it is now possible to use micro beams and combine diffraction rapidly collected from many different areas. In the case of the Li_xCoO_2 battery 16 different orientations were collected in less than 2 secs and the pixel by pixel medians of the images collected by the CCD camera could be used to reduce the influence of the electrodes. One-dimensional powder patterns from 2 D images can thus be produced with sufficient precision to obtain accurate time-resolved behaviour of the phase fractions during the working cycle of the battery. The structures of the phases that are stable only under applied voltage

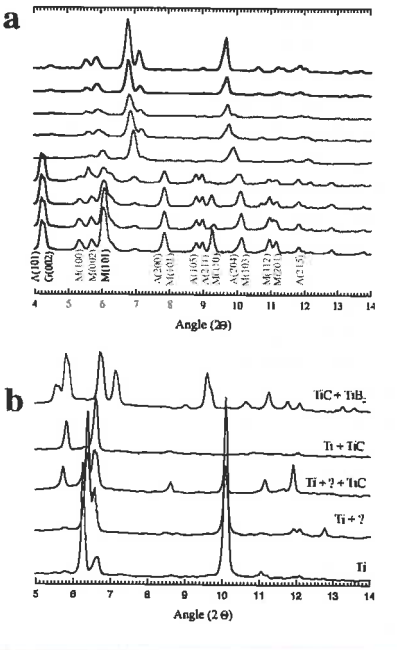

▲ **Fig. 5:** (a) The diffraction pattern during the reaction between A (anatase), G (graphite) and M (magnesium). The time resolution is 0.65 msec. (b) The diffraction patterns captured while the reaction between the metals take place. The time interval is 0.65 ms.

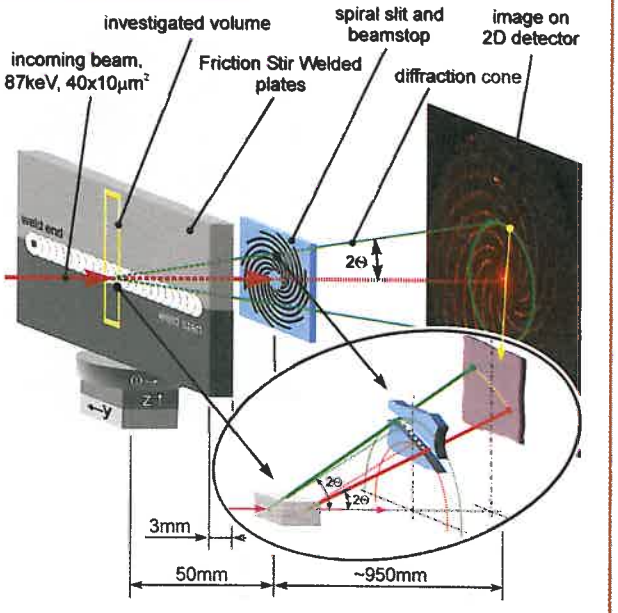

▲ **Fig. 6:** Schematic of the experimental setup with spiral slit and online image plate scanner on ID15B.

showed the existence of intermediate phases as well as the terminal layered CoO_2 structure. Figure 4 gives the diffraction phases during *in situ* reduction of the Li_xCoO_2 battery with the different rhombohedral, monoclinic and triclinic phases indicated.

The highest time-resolution for irreversible reactions so far (10-30ms) has been obtained in the study of self-propagating high temperature synthesis (SHS). SHS is based on the characteristic of highly exothermic reactions to sustain themselves following an initiation by relatively mild conditions. These reactions typically proceed as reaction fronts with speeds of up to 25cm/sec under temperatures up to 5000C. An example is given by Contreras *et al.* 2004 where the production of TiC and TiB_2 was studied via two routes: from elements and from oxides. The reactions were monitored by 0.2601 Å X rays *in situ*. The starting powders were compacted to cylindrical pellets and the reaction was started by external ignition at the bottom of the pellets. The X- ray beam was focused on the central part of the pellet and the reaction process was recorded as the reaction front passed the probing X-ray beam. The bulk process was followed by recording the diffraction in transmission by a CCD camera. The detailed process could be recorded and showed that the entire process took place during less than 0.1 second. The different synthesis routes produced different final microstructures that depended on the starting conditions. The particle size when pure elements were used was 10 µm whereas the reaction using oxides and Mg had sub-µm microstructure. Fig. 5 gives the diffraction patterns during the critical phases of the reactions.

Combined diffraction and imaging

High spatial resolution

The mapping of residual stresses in components is essential in providing a roadmap for future failure modes in materials and a detailed knowledge of their distribution can indicate potential alleviating processes, which may lengthen component lifetime and avert catastrophic failures such as fractures in railroad tracks or airplane turbine blades. Until recently only destructive methods or methods with large measuring gauges have been employed. Recent developments at the high energy synchrotron facilities have now produced highly penetrating micro-focus beams with measuring gauges down to ~5*5*50 µm³. The experimental set-ups with CCD cameras or narrow receiving slits and micro-precision translation tables now give spatial resolution on the µm scale. High precision lattice parameters with $\Delta d/d \sim 10^{-6}$ can thus be determined with the small measuring gauge and excellent spatial resolution. A recent example of a novel strain and phase-mapping technique is given by Martins *et al.* 2003 in their depth resolved investigation of friction stir welding. Friction stir welding is a new method for solid welding using a spinning tool forced along a joint line. This new method can overcome problems such as weld porosity, use of filler materials and cracking in the heat-affected zone. In this study the bulk investigation of several mm thick Al plates was performed, and the depth resolution was obtained by a spiral slit assembly.

The experimental set up is illustrated in Fig. 6 and the resulting distribution of the Si phase and the residual micro strain is given in Fig. 7 for this weld of a single phase Al alloy and an $AlSi_{10}Mg$ phase.

Multi-crystal techniques

The excellent spatial resolution now available opens up entirely new opportunities for studying dynamical phenomena at the mesoscopic level. Surprisingly theoretical understanding of many fundamental materials processes, such as recrystallisation and deformation, relies on models that have built in assumptions such as sample homogeneity and absence of grain-grain interactions. The new experimental facilities can now test these assumptions. An example is given by Offerman *et al.* 2002 in their study of grain growth following phase transformations in a steel sample. Using the spatial resolving power of the synchrotron beam it was shown

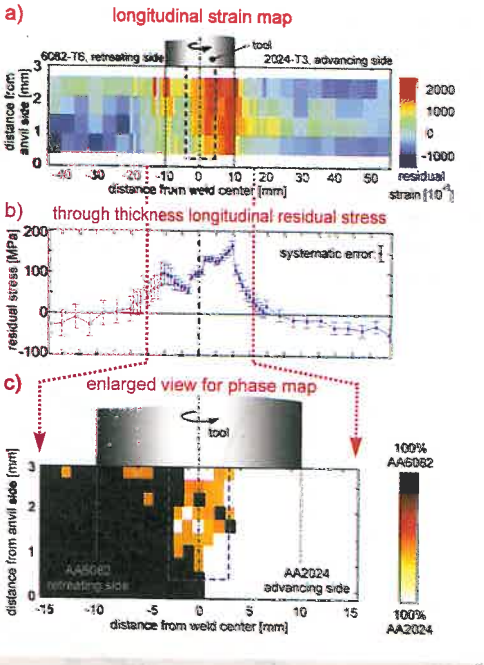

▲ **Fig. 7:** (a) Depth resolved residual macrostrains in longitudinal direction (parallel to weld). (b) through thickness longitudinal residual stress component, calculated from the strain measurements in three dimensions. (c) enlarged view of the distribution of the plate material (AA6082 and AA2024) in the stirring zone.

that four different growth mechanisms were present in ferrite and these were correlated with the local environment of the grains indicating that the present models are far from adequate. Fig. 8 shows the integrated intensity of 5 grains near the cube orientation shown as a function of annealing time. At present several hundred different grains can be monitored simultaneously. This method of simultaneous determination of orientation within a bulk sample (Lauridsen *et al.* 2000) gives interesting access to the mesoscale. It is now possible, via tracking techniques, to map out grain boundaries with resolutions down to 5 μm and to follow kinetics and dynamics of groups of individual grains during processes such as heating, torsion etc.

Industrial application of Bragg diffraction imaging (X-ray topography)

Figure 9 shows the image recorded using the 444 Bragg diffracted beam from a flux-grown platelet-shaped gallium-substituted yttrium iron garnet crystal ($Y_3Ga_xFe_{5-x}O_{12}$, with x~1, Ga-YIG). These Ga-YIG crystals are grown to produce hyper-frequency resonators. It was observed that some of these crystals exhibit spurious modes, which are very detrimental to their performance. This X-ray diffraction topographic investigation was therefore performed to identify the crystal defects present on some of the resonators, produced during growth, which are responsible for these spurious modes. Many types of defects are observable on the topographs, and one of them, the dissolution bands, appeared to be the origin, through the occurrence of "closure-like" magnetic domains, of these modes.

Future developments

The above examples give only a few insights of possible studies of industrial phenomena using diffraction and imaging at the synchrotrons.

X-ray microtomography is an invaluable tool to obtain 3D data on a large variety of materials. The use of modern synchrotron radiation sources opens up new possibilities, with "fast tomography" to investigate the evolution of a system when varying an external parameter (time, temperature, stress, etc.) and/or improved spatial resolution, going down to the 100 nm range. In addition phase images reveal phenomena hardly visible by other means.

Other areas include the rapidly expanding field of high-pressure diffraction where micro- focussed beams and laser-heating capabilities open up new experimental routes to studies of synthesis

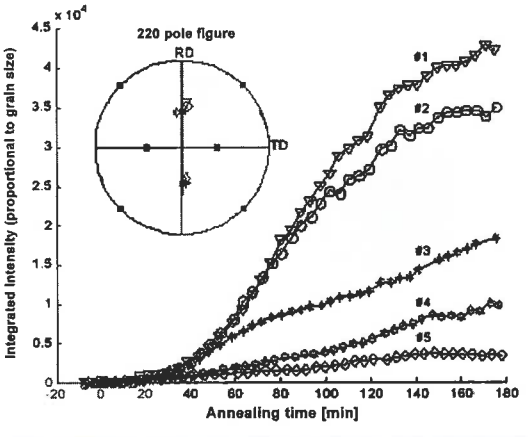

▲ Fig. 8: The integrated intensity of five grains near the cube in steel as a function of annealing time

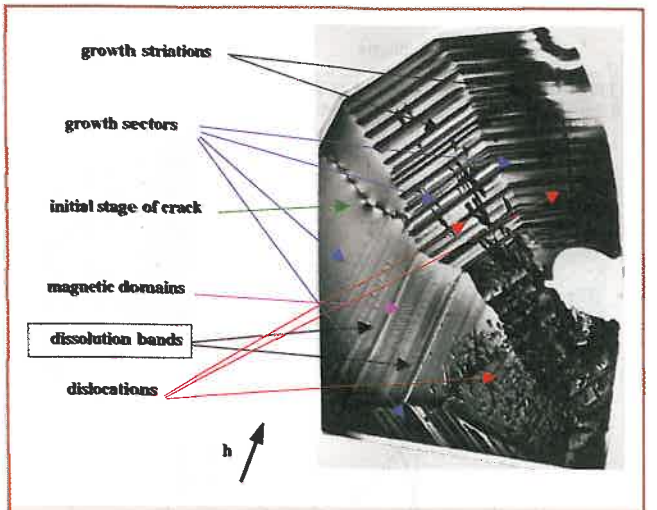

▲ Fig. 9: Topograph of a flux grown Ga-YIG crystal.

and equation of states under non-ambient conditions such as megabars of pressure and several thousands of degrees of temperature.

High-resolution powder diffraction is advancing rapidly and *ab initio* structure determinations of very large structures can now be performed on materials, which cannot be obtained as single crystals.

The current trend in instrumentation development will in the near future give access to nanometre size beams. This leads to another type of image through the use of X-ray microbeam-based scanning imaging approaches, probing for instance the fluorescence or the absorption near absorption edges. The diffraction experiments will more and more be combined with complementary techniques such as imaging or Raman spectroscopy, by performing simultaneous observations. Development in detector technology will further advance the time- and space-resolving aspects of the experiments.

About the authors

Åke Kvick graduated from Uppsala University in 1974. Work on hydrogen bonded systems, zeolites and time-resolved studies with neutrons and X-rays. Scientist at Brookhaven National Lab. 1980-1989. From 1989 work at the ESRF on synchrotron radiation diffraction; presently Head of Materials Science Group and editor of J. Synch.Rad.

José Baruchel graduated in Physics at the University of Grenoble. From 1971 to 1991, work on magnetic domains and nearly perfect crystals, with X-rays and neutrons. From 1991, work at the ESRF on synchrotron radiation imaging (topography and tomography); presently Head of the X-ray Imaging Group.

References

Bontaz-Carion J., Nicollet M., Manczur P., Pellegrini Y.-P., Boller E., Baruchel J. *Dynamic damage in metal: porosity as a test for damage models*, in A. Chiba, S. Tanimura and K. Okamoto eds., Impact Engineering and Application, Proc. 4th Int. Symp. on Impact Engineering, pp.633-638 , Elsevier, Oxford (2001).

Buffière J.Y., Maire E., Cloetens P., Lormand G. and Fougères R., *Characterization of internal damage in a MMCp using synchrotron phase contrast microtomography*, Acta Mater. **47**, 1613-1625 (1999)

Cloetens P., Ludwig W., Baruchel J., Guigay J.P., Rejmankova-Pernot P., Salomé-Pateyron M., Schlenker M., Buffière J.Y., Maire E., Peix G., *Hard*

X-ray phase imaging using simple propagation of a coherent synchrotron radiation beam. J. Phys. D: Appl. Phys.**32**, A145-A151 (1999a)

Cloetens P., Ludwig W., Baruchel J., Van Dyck D., Van Landuyt J., Guigay J.P., Schlenker M., *Holotomography: quantitative phase tomography with micrometer resolution using hard synchrotron radiation X-rays*, Appl. Phys. Lett. **75**, 2912-2914 (1999b)

Contreras L., Turillas X., Vaughan G.B.M., Kvick Å., Rodriguez M.A. *Time-resolved XRD study of TiC-TiB_2 composites obtained by SHS.* To be published (2004)

Elliott J.A., Windle A.H., Hobdel J.R., Eeckhaut G., Oldman R.J., Ludwig W., Boller E., Cloetens P., Baruchel J., *Foam compression by microtomography*, J. Mat. Science, **37**, 1547-1555 (2002).

Lauridsen E.M, Juul Jensen D. ,Poulsen H.F. Lienert U., *Kinetics of individual grains a during crystallisation.* , Scripta Materialia, **43**, 5561-566(2000).

Martins R.V, Honkimäki V., *Depth resolved investigation of friction stir welds using a novel strain and phase mapping technique* , Texture and Microstructure, **35**, 145-152(2003).

Morcrette M., Chabre Y., Vaughan G.B.M., Amatucci G., Leriche J.B.,Patoux S., Masquelier C., Tarascon J.M. *In situ x-ray diffraction techniques as a powerful tool to study battery electrode materials.* Electrochimica Acta, **47**, 3137-3149 (2002)

Offerman S.E, van Dijk N.H, Sietsma J., Grigull S., Lauridsen E.M, Margulies L., Poulsen H.F., Rekveldt M.Th., van der Zwaag S. *Grain nucleation and growth during phase transformations.*Science ,**298,** 1003-1005(2002).

Rüegsegger P., Koller B.and Müller R,. *A microtomographic system for the non destructive evaluation of bone architecture*, Calcif. Tiss. Int., **58**, 24-29 (1996).

Sasov A. and Van Dyck D., *Desk-top microtomography: gateway to the 3D world*, European Microscopy and Analysis, pp. 17-19 (1998).

What is your strategy for Framework 6?

Sean McCarthy, Managing Director of Hyperion Ltd.

How many research organisations have a formal written strategy for Framework 6? How many individual researchers have a personal strategy for Framework 6? This article presents a checklist for the writing of a simple but practical strategy for Framework 6.

An organisation's strategy for Framework 6

The following are examples of statements of objectives that could be used in a research organisation's strategy for Framework 6. They are based on actual discussions with research organisations on their Framework 6 strategies. (The comments in brackets are actual quotations from research managers)

- To access European Union Funding for research activities. One of the problems with this simple objective is that the researchers may concentrate on obtaining any contracts rather than focussing on the research priorities of the organisation.
- To establish the research group as the European (or International) scientific leader in a scientific area ('to be the best in our field'). It is important that the scientific areas are well defined (a niche within an niche). For example, ' to be the world leader in the simulation and design of photovoltaic (solar) systems'.
- To access new technologies relevant to the organisation's areas of excellence ('to avoid missing the train').
- To work with the best research partners in the European Union. ('to be the preferred partner of the best scientists in our field')
- To provide better education and training to graduates and post-graduates. ('We want our graduates to excel in any interview, anywhere in the world')
- To promote the organisation's scientific and technical excellence to the scientific/technical community ('more conferences, more publications, more website hits...')
- To ensure the research results are used by enterprises and society ('getting value from our research efforts')
- To provide relevant support to researchers ('To streamline the process of proposal writing, contract negotiation and contract management/administration').

The strategy should also describe the activities that the organisation will NOT undertake in Framework 6. For example:

- Specific tasks in the contract. (One University clearly informed its researchers that 'we will not act as main contractor in Framework 6 contracts').
- No subcontracting. (' We will utilise only internal resources in the contracts')

A strategy for individual researchers

An individual researcher (or a small research group) should have a strategy covering all of the following issues:

- Which is the scientific niche (or even a 'niche within a niche') where the researcher's expertise is the best and where it complements that of researchers from other research centres. This requires clear identification.
- Which Framework 6 Priorities (sub-programmes) are relevant

to the researcher? All of the sub-programmes—not just the main programmes—should be identified.
- Which Instruments (types of contracts) will be used? A simple strategy could be the following: ' The research group will focus on Integrated Projects and Networks of Excellence. STREPS will be used to explore future research topics. Specific Support Actions will be used to fund workshops and small conferences. Coordination Actions will be used to fund research networks. Marie Curie Fellowships will be used to hire researchers or to fund PhD students. The Research Infrastructure instrument will be used to access research facilities'.
- Which 'Calls for Proposal'? Each programme will have (typically) one call for proposals each year. An example of a strategy could be: In 2004 the research group will focus on Specific Support Action to establish links with potential partners. In 2005 the group will set up a Coordination Action to establish a formal network with other research organisations. This network should lead to an Integrated Project or a Network of Excellence in 2006.
- What Role in the Project? Scientific Coordinator? Main contractor? Work-package leader? Consortium Manager? Exploitation Manager?
- Which partners? This is the most critical issue and will require the most thorough analysis. Which companies and in particular which SMEs (Small and Medium Enterprises) could be included in the project? Which partners from the Candidate Countries should be included?
- What support staff is available? Examples include: Who will write the Gender dimension of the proposal? Who will take care of the ethical issues, the consortium agreement etc.?
- Which sources of information? Framework 6 proposals require arguments in science, economic relevance, social relevance, relevance to European Union policies etc. Which are the best sources of information for these sections of the proposal? For this information see www.hyperion.ie/framework6websites.htm
- Which templates can be used to streamline the process of proposal writing? Sample templates can be found on: www.hyperion.ie/templates.htm

From strategy to people

Framework 6 is about people. It is not just about EU institutions, websites and proposal documents. The researchers who are successful in Framework 6 contracts are active in a wide variety of EU activities. They network and more importantly they maintain networks. The following is a simple strategy for action by a researcher to identify the key individuals in their scientific area in the EU.

1. Identify the relevant individuals in the European Commission. The organisation structure can be found on: http://europa.eu.int/comm/dgs/research/organisation_en.html
2. Identify the researchers that are already partners in EU R&D contracts in your area. These can be found on the search engine in http://dbs.cordis.lu/fep/FP5/FP5_PROJl_search.html
3. Identify the individuals that are working as experts to the European Commission. In particular, identify the researchers that are involved in advisory committees or those who write policy documents on scientific topics. Examples of all Framework 6 topics can be found on www.hyperion.ie/fp6websites.htm
4. Join the relevant EU Research Associations. Examples can be found on www.hyperion.ie/euassociations.htm
5. Join relevant Thematic Networks that were funded under Framework 5. These can be found on: http://dbs.cordis.lu/fep/FP5/FP5_PROJl_search.html by searching under THEMATIC NETWORK.
6. Researchers should promote their expertise at EU conferences, exhibitions and in relevant magazine. This can be done through Thematic Networks and European Research Associations (listed above).
7. Participate in Framework 6 evaluations to learn the process of proposal writing and proposal evaluation. The call for experts can be found on www.cordis.lu/fp6/

Conclusion

Strategies are useless pieces of paper unless implemented. A strategy is not a once in a lifetime exercise – it must be regularly updated to reflect changes in internal research priorities, changes in funding rules or changes in funding priorities. It is important that a general strategy exists and that it is communicated throughout the research organisation.

Research organisations and individual researchers should be able to answer the following questions:
- How will the success of participation in Framework 6 be measured?
- How will the failure of involvement in Framework 6 be measured?
- What is the greatest concern of the organisation regarding Framework 6?
- What are the limitations of the researchers and the limitations of the organisation when participating in Framework 6?

If the researchers cannot answer these questions they may be travelling in the wrong direction.

The best strategy will always involve producing the best science and working with the best partners.

About the author

Dr. Sean McCarthy (sean.mccarthy@hyperion.ie) is Managing Director of Hyperion Ltd. Hyperion specialises in the development of training courses for research managers. Full details of their training courses can be found on www.hyperion.ie. Hyperion's clients can be seen on www.hyperion.ie/clients.htm

Framework 6 proposals feedback

EPN is undertaking a survey to assess the level of involvement of its readers in Framework 6 and to compile a short report on the experiences of people who submitted proposals during the first year of the programme. Sean McCarthy of Hyperion Ltd. will analyse the replies and present the results in a future edition of EPN. This information will be valuable to EPN readers in the planning of future research proposals.

1. Did you submit a proposal to Framework 6?
2. If you did not submit a proposal, then what were your reasons?
3. What was the most difficult part of the proposal to write?
4. Did you participate as a partner or as the coordinator of the proposal?
5. How much effort (in person days) was involved in participating in the proposal?
6. Have you any recommendation you would like to make to the European Commission regarding proposal writing for Framework 6 (and future Framework programmes)?

Please email your replies to sean.mccarthy@hyperion.ie before 28th April 2004. Participation of EPN readers will be greatly appreciated.

Chromatic effects near a white-light vortex

Jonathan Leach and Miles J Padgett
University of Glasgow, University Ave, Glasgow, UK

Phase singularities are common throughout optical physics [1-3]. They occur at points or regions of undefined phase, the consequence of which is that the light field has zero intensity. Phase singularities in white-light sources have been modelled and studied experimentally, producing dramatic chromatic effects [4-9]. Recently, these chromatic effects were predicted to exist in the case of beams containing optical vortices [10,11]. We have experimentally observed these distinctive effects by looking closely at the centre of such beams, produced by a spatially coherent white-light source and a computer generated hologram [12].

A simple example of a singularity is that of a spiral staircase. However, it is not possible to accurately describe the center height, leading to a singularity at the center of the staircase.

The example of a spiral staircase is particularly illustrative when considering beams that contain optical vortices. The steps that spiral around the center of the staircase are equivalent to surfaces of constant phase around the beam's axis. This helical phase structure means the phase on the beam's axis is undefined resulting in a phase singularity. The corresponding intensity zero produces a characteristic ring or "doughnut" intensity profile of the beam.

In our case, we are interested in phase singularities of not monochromatic light but of white-light, for example a tungsten halogen bulb. In order to get helical phase fronts, we produced a spatial coherent white-light beam by passing light from the bulb through an optical fiber and collimating the output. The helical phase structure was then added to the beam by reflecting it off a computer-generated hologram. The design of the hologram resembled that of a diffraction pattern but with an additional fork dislocation on the beam's axis. The first order diffracted beam has the desired helical phase structure. After the hologram, each spectral component of the source was recombined and made co-axial with a low dispersion prism. The relative direction of the components and thus spectral spread of the source could then be controlled by the computer-generated hologram.

As the chromatic effects occur in the center of the beam where there is very little light, they are very hard to observe. The effects are subtle and can only be revealed by amplifying the colours. The technique used is referred to as a "chromascope". This is a colour correction such that at every pixel in the image, the RGB values are

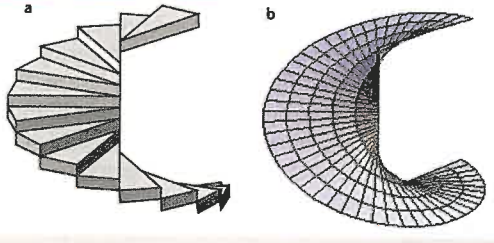

▲ **Fig. 1:** Examples of singularities. a). A spiral staircase where the height in the middle is undefined. b). The helical phase fronts of a beam with an optical vortex.

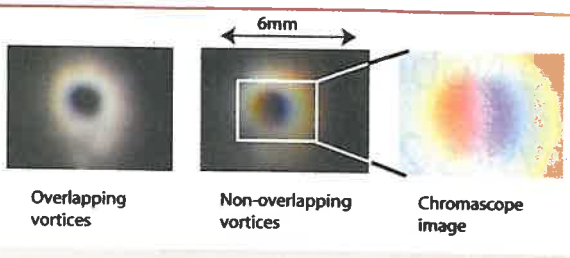

▲ **Fig. 2:** Experimental results.

increased to make the largest of them fully saturated whilst maintaining their ratios.

Figures 2 and 3 show our experimental results. Figure 2 contrasts the case where the optical vortices for each spectral component in the white-light source are overlapping and not overlapping. When the vortices are not overlapping, the chromascope image reveals the chromatic patterns at the center of the beam. Figure 3 compares the experimental results to the theoretical predictions made by Berry. In both cases, the transition across the image from red to blue is clear. Note that neither image contains any green.

Although the detailed form of these patterns is complicated, the underlying principles, which give rise to these chromatic effects, can easily be understood. For each spectral component, there is a corresponding intensity zero. The dispersion of the vortices produces a line along which specific spectral components are not present. At one extreme, there is no blue component, at the other, there is no red component, and in the center, there is no green. This gives rise to a dominance of the complimentary colours, cyan, magenta (purple) and yellow. The absence of any green region over the entire beam cross-section is explained since it would require the red and blue vortices to be coincident, which they are not.

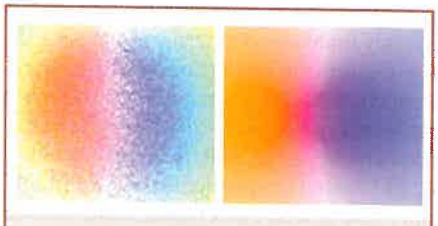

▲ **Fig. 3:** A comparison of the experimental results to the theoretical predictions (Berry, *New. J. Phys.*, 4 66).

This paper is a summary of an article published in NJP. Full version available at: http://www.iop.org/EJ/abstract/1367-2630/5/1/154

References

[1] Nye J.F and Berry M.V., 1974 *Proc. R. Soc.* A, **336** 165–190

[2] Nye J.F 1999 *Natural Focusing and Fine Structure of Light: Caustic and Wave Dislocations* (Bristol: Institute of Physics Publishing)

[3] Soskin M.S and Vasnetsov M.V, 2001, *Prog. Opt*,. **42** 219–276

[4] Gbur G., Visser T.D. and Wolf E, 2002, *Phys. Rev. Lett.*, **88** 013901

[5] Gbur G., Visser T.D. and Wolf E 2002, *J. Opt. Soc. Am.*, **19** 1694–1700

[6] Foley J.T. and Wolf E., 2002, *J. Opt. Soc. Am.*, **19** 2510–2516

[7] Ponomarenko S.A. and Wolf E., 2002, *Opt. Lett*,. **27** 1211–1213

[8] Popescu G. and Dogariu A., 2002, *Phys. Rev. Lett.*, **88** 183902

[9] Schouten H.F., Gbur G., Visser T.D. and Wolf E., 2003, *Opt. Lett.*, **28** 968–970

[10] Berry M.V., 2002, *New J. Phys.*, **4** 66

[11] Berry M.V., 2002, *New J. Phys.*, **4** 74

[12] Leach J. and Padgett M.J., 2003, *New J. Phys.*, **5** 154

The Nobel Prize in Physics 2003

Gianni Blatter and Vadim Geshkenbein,
Theoretische Physik, ETH Zürich, Switzerland

The phenomenology of condensed quantum liquids has been the winning theme in last year's Nobel competition—Alexei A. Abrikosov (Argonne National Laboratory), Vitaly L. Ginzburg (Lebedev Institute in Moscow), and Anthony J. Leggett (University of Illinois at Urbana) share the 2003 Nobel prize in physics for their "pioneering contributions to the theory of superconductors and superfluidity." Their names are added to the illustrious list of Nobel laureates in the field of low temperature physics.

Superconductivity/fluidity has always been the most glamorous topic in condensed matter physics. The milestones characterizing the field start with the discovery of superconductivity in mercury by Kamerlingh Onnes in 1911. In 1938, the superfluid phase of ^{4}He was found by Kapitsa in Moscow and independently by Allen and Misener in Cambridge. Since metallic mercury transports electric current free of dissipation the original name 'super *conductor*' stuck; liquid He is uncharged and hence the dissipation-free mass flow is termed super*fluidity*. While the superfluid properties of bosonic ^{4}He were quickly understood in terms of a condensation into a macroscopic quantum state (Landau, 1941), the microscopic origin of superconductivity remained a puzzle over half a century, until Bardeen, Cooper, and Schrieffer (1957) proposed a pairing mechanism allowing bound fermions to condense. This paved the way for the theoretical prediction that fermionic ^{3}He should become superfluid as well, but it took another decade until Lee, Osheroff, and Richardson observed the superfluid phases of ^{3}He in 1972. The unexpected discovery of high-temperature superconductors by Bednorz and Müller in 1986 defined the most prominent research direction in condensed matter physics for the decade to follow. Last year the spectacular insights that follow from phenomenological theories have been properly recognized.

The Ginzburg-Landau Theory

Upon cooling to sufficiently low temperatures, electrons or atoms must lose entropy and organize themselves into a more ordered state. In doing so, the system undergoes a reduction of symmetry, the central idea of Landau's phenomenological theory of phase transitions dating back to 1937. The symmetry breaking is captured by an *order parameter*, whose nature is most obvious in a ferromagnet where it quantifies the material's magnetization. Also, the idea of Bose-Einstein condensation into a macroscopically occupied quantum state suggests a superfluid order parameter in the form of a complex wave function Ψ. Because of the Pauli principle, it remained completely unclear, however, what could be a proper order parameter for the fermionic electron system in a superconducting metal and it required the remarkable intuition of Ginzburg and Landau to propose an order parameter in the form of a complex electronic wavefunction $\Psi = \sqrt{\rho}\exp(i\varphi)$. The Ginzburg-Landau free energy functional, which they constructed based on this order parameter set the foundation for the complete phenomenological understanding of superconducting materials.

Quite astonishingly, the rich phenomenology of the superconducting state could be quantitatively described without knowledge of the underlying microscopic mechanism responsible for the condensation in the first place. Early work of Gorter, Casimir, and the London brothers, explained numerous thermodynamic and electromagnetic aspects of the superconducting state. In particular, the London equation relating the superconducting current $\mathbf{j}_s$ to the vector potential $\mathbf{A}$ via the superconducting density ρ_s, $\mathbf{j}_s = \rho_s\mathbf{A}$, properly explained the Meissner-Ochsenfeld effect, the complete expulsion of a magnetic field from the interior of a superconductor. However, discrepancies with experiment remained, particularly in films subject to a parallel magnetic field where the expression for the critical field $H_{c\|}$ destroying superconductivity failed. Furthermore, the London theory was unable to provide a positive surface energy for the superconducting-normal interface, hence a basic ingredient to Landau's intermediate state (1937) remained unexplained. These practical shortcomings were overcome in the 1950 paper of Ginzburg and Landau. In setting up their famous energy functional they allowed for the presence of a magnetic field. The minimal gauge invariant coupling $|(-i\hbar\nabla-(e/c)\mathbf{A})\Psi|^2$ led them to the subtle remark that '*e* is *a* charge, which there is no reason to consider as different from the electronic charge', thus accepting the possibility that it may take a different value. The ability to incorporate variations in the Ψ-field due to boundary conditions, external magnetic fields, and currents, allowed them to remedy the deficiencies of the London theory. With the Ginzburg-Landau energy functional, the vector potential $\mathbf{A}(\mathbf{r})$ properly described within the London theory got its partner field, the macroscopic wave function $\Psi(\mathbf{r})$, thus providing the complete phenomenological description of a charged quantum fluid. However, it still required Gorkov's derivation from the microscopic BCS theory (1959) until the Ginzburg-Landau equations acquired their definitive status with an effective charge 2e.

With the appearance of a second (Ψ-) field a new dimensionless parameter comparing the relative 'stiffness' of the two fields enters the theory: the Ginzburg-Landau parameter $\kappa = \lambda/\xi$ measures the ratio in lengths associated with changes in the electromagnetic response (the London penetration depth λ) and in the superconducting density (the coherence length ξ). The limiting value $\kappa = 1/\sqrt{2}$ separating superconductors with positive surface energy ($\kappa < 1/\sqrt{2}$) from those with negative surface energy at large $\kappa > 1/\sqrt{2}$, was properly identified and the instability associated with the negative surface energy was noted, but the consequences were not pursued. At the time, superconductivity had been observed in elementary superconductors characterized by a small κ, hence Ginzburg and Landau decided that 'since from experimental data it follows that $\kappa \ll 1$ ... another limiting case when $\kappa \to \infty$ does not offer any intrinsic interest (and) we shall not discuss it'.

Type II Superconductors

It remained for Alexei Abrikosov to uncover the scientific gold mine that opened up with the 'superconductors of the second group' involving large κ, nowadays called type II superconductors. Abrikosov's first contact with these 'unconventional' superconductors dates back to the early fifties, when Nikolay Zavaritskii changed the fabrication mode of his thin Sn and Tl films, keeping the substrate at low temperatures in order to improve their homogeneity. While the behavior of his previous room temperature evaporated films was in good agreement with theory, the new ones deviated strongly. This led Abrikosov and Zavaritskii to propose that these new films belong to the 'second group' of superconductors with $\kappa > 1/\sqrt{2}$ and indeed their critical field matched well the theoretical result found by Abrikosov in 1952. The breakthrough came in 1957, when Abrikosov obtained the basic phenomenological description of type II superconductors in a single stroke. The instability noticed

▲ **Photographs:** From left to right: Abrikosov, Ginzburg, and Leggett receiving the Nobel Prize in Physics 2003.

by Ginzburg and Landau allowed the magnetic field to enter the superconductor without destroying it. This leads to the appearance of an interesting new thermodynamic phase, the mixed or Shubnikov phase, where superconducting and normal regions peacefully coexist. The normal regions appear in the cores (of size ξ) of vortices binding individual magnetic flux quanta $\Phi_0 = hc/2e$ on the scale λ, with the charge '$2e$' appearing in Φ_0 a consequence of the pairing mechanism; since $\lambda > \xi$, the vortices repel and arrange in a stable lattice, nowadays named after its inventor Alexei Abrikosov. In his 1957 paper, Abrikosov derived the periodic vortex structure near the upper critical field H_{c2}, where the superconductivity is totally suppressed, determined the magnetization $M(H)$, calculated the field H_{c1} of first penetration, analyzed the structure of individual vortex lines, found the structure of the vortex lattice at low fields, and compared his findings with experiments on what appeared to be the first observation of this novel mixed state, the $B(H)$ curves measured on Pb alloys by Shubnikov, Khotkevich, Shepelev, and Riabinin in 1937. Although this already makes an impressive list, the phenomenology of type II superconductors continued to develop for many years. It turns out that all technologically useful superconductors are 'of the second group'; these materials smoothly incorporate the large magnetic fields appearing in most technological applications, hence they 'bend' rather than 'break' under the action of fields and currents. In particular, the cuprate high temperature superconductors (discovered by Bednorz and Müller in 1986) are strong type II materials exhibiting an amazing variety of vortex phases with novel properties. Meantime, the Abrikosov lattice has undergone a 'metamorphosis' to the field of Vortex Matter, the filigrane arrangements formed by vortex-lines residing within conventional matter made of atoms and electrons.

As so often in the field of superconductivity it took many years to understand the rich and complex phenomenology of these materials. Political events also hampered the developments : in 1937 Shubnikov was accused of 'anti-Soviet activity' and sentenced to death; the same accusation led to the imprisonment of Landau in Moscow. Thus, Shubnikov's 1937 results on the mixed state failed to catch the attention of the community for 20 years. Similarly, the cold war hampered the diffusion of the amazing achievements of Russian theoreticians in the west.

Superfluid ^{3}He

^{3}He is an uncharged quantum fluid with a repulsive interatomic interaction at short distances favoring pairing in a finite angular momentum state. The order parameter field then assumes a complex structure incorporating additional internal degrees of freedom: the unconventional pairing involves atoms with parallel spins (triplet channel with $S = 1$) and orbital momentum $L = 1$. As a result, the superfluid phase is anisotropic, with $\hat{\mathbf{d}}$ and $\hat{\mathbf{l}}$ two directions associated with the additional spin- and orbital degrees of freedom. Hence cooling ^{3}He down to low temperatures, leads not only to the breaking of gauge symmetry but also of the rotational symmetry in spin- and orbital space, thus requiring a macroscopic wavefunction with a tensorial structure involving 3×3 complex components (at least in principle). In practice, the lowest energy state is isotropic, with the spin- and orbital angular momenta adding to zero (the BW state first found by Balian and Werthamer in 1963). Its excitation spectrum exhibits a constant energy gap just like a conventional BCS superconductor. Even earlier, Anderson and Morel had proposed an anisotropic state, with zero energy gap along the $\hat{\mathbf{l}}$-axis (the AM state). But another decade passed until Lee, Osheroff, and Richardson finally observed the superfluid phases of ^{3}He in 1972, an A-phase at elevated temperatures and pressures and a B-phase in the remainder of the low temperature phase diagram. It was Anthony Leggett who unravelled the puzzle of interpreting the experimental data with the correct theoretical picture. The NMR (nuclear magnetic resonance) data identifying the new phases exhibited sharp resonance frequencies, unexpectedly shifted in the A but not in the B phase, which Leggett explained in terms of a new 'spontaneously broken spin-orbit symmetry'. While this symmetry is trivially broken in the AM state through selection of specific directions $\hat{\mathbf{d}}$ and $\hat{\mathbf{l}}$, the situation is more subtle for the isotropic BW state, where neither $\hat{\mathbf{d}}$ nor $\hat{\mathbf{l}}$ but only their relative orientation is fixed. This subtly broken rotational symmetry manifests itself only in the dynamical response. Soon after the discovery of the new superfluids, Leggett presented his explanation for the observed shift in terms of a dipole field enhanced by the macroscopic alignment of nuclear spins and predicted the existence of additional longitudinal modes in the AM and BW phases. He identified the AM state as a possible candidate for the observed A phase but noted the competition with the lower energy BW state. This led Anderson and Brinkman (1973) to reconsider the AM state and they demonstrated its stabilization due to the feedback effects of the condensation on the interparticle interactions (nowadays the ABM state carries the initials of all three authors). Finally, Ambegaokar and Mermin (1973) identified the third phase (termed A1) appearing at finite magnetic fields as the first magnetic superfluid.

In retrospect, the complexity of ^{3}He teaches us an interesting story. At first sight ^{4}He and ^{3}He are two fluids characterized by the same isotropic Lennard-Jones type interaction. The source of their difference lies in the absence of one neutron in the nucleus of a ^{3}He atom which is enclosed in a rigid electronic shell governing the interaction between atoms. Still, the low temperature properties of the two fluids are as different as one could imagine, owing to the quantum-mechanical properties of their light constituents. One may wonder what ingenuity it would take for an observer living at low temperatures and confronted with this complexity to guess the correct simple high-energy Hamiltonian responsible for this diversity of phases. This inverse task, guessing the correct "high-energy Hamiltonian" from observations at low energies, is analogous to the central problem facing the particle physics community. In condensed matter theory the program of deriving the correct microscopic Hamiltonian from experimental observations has been carried out many times, with the BCS Hamiltonian serving as a prominent example. One should appreciate, however, the amazing insights that phenomenological low-energy theories, such as those introduced and used by Ginzburg, Abrikosov, and Leggett, have contributed to our understanding of the world we live in.

Acknowledgements

We thank M. Rice, D. Vollhardt, and P. Wölfle for discussions.

Out of the Ivory Tower and into the Streets

French researchers have entered into the political arena with the "Let's Save Research" petition. The first paragraph reads "At the dawn of the 21st century, France needs dynamic research. Such activity is necessary for future innovation, the economic development of our country, as well as its cultural influence abroad. In the current economic context, countries that do not maintain a top-flight research capacity will fail to keep up with the increasingly rapid economic changes related to the production of knowledge. Even more seriously, moreover, they will fast become incapable of training young generations in a competitive manner. They will thus enter a condition of economic dependency that will be difficult to reverse." A link to the full text in English is available at: http://recherche-en-danger.apinc.org/ .

Researchers in France have been very critical of the budget decisions, and decided that it was time to mobilise public support to influence politicians in France. At present, the petition has over 54,000 signatures. The petition highlights the role of scientific research in society, the necessity for fundamental research, as well as real career opportunities for researchers, and the necessity to attract and keep talented young people.

Beginning with a large demonstration in Paris on 29 January 2004, where over 10,000 people were in the streets. Other demonstrations have been organised throughout France, from Bordeaux to Strasbourg to sensitize the general public to the plight of researchers in France.

A similar situation has occurred in Switzerland, when the University Board announced in January 2004 that it wanted to close down the Astronomical Institute of the University of Basel. Closing the Institute would break the tenure of two professors and lead to the lay off of a number of other highly accomplished staff. It will also have an impact on physics, as astronomy lectures offered as part of physics curriculum motivate young people to take up physics studies. This seems counterproductive when the number of physics students is insufficient to maintain our highly technological civilisation.

A petition for maintaining the Astronomical Institute has been signed by several thousand persons from the general public. Colleagues from around the world have written letters of protest because the Institute's research and teaching is highly rated by their peers. The Institute has issued a position paper, demonstrating the flaws in the reasons motivating the Board's decision. (full-text in German is available at: http://www.astro.unibas.ch/indexengl.shtml)

Science policy concerns not only scientists. It is often the scientists themselves who have the deepest understanding of what the impact of bad policy decisions will mean to the society at large. Scientists have a duty to inform and shape public opinion on questions of science policy.

Update

Since the writing of this article 2000 French researchers have resigned from their administrative positions in protest of the refusal of the French Government to hire 550 young researchers.

Yet another ITERation to select a site for a world fusion project

J. Lister, EPS Plasma Physics Division

The fusion community was holding its breath once again on the 20th December when a ministerial meeting between the six ITER parties took place in Washington. The role of the meeting was simply to choose between two sites to host the ITER fusion project. Both Rokkasho in northern Japan and Cadarache in southern France sites had passed the criteria of an international site selection committee. The EU selection between Cadarache and an alternative European site in Vandellos in Spain had recently been made, allowing this one-on-one contest to take place. During the ministerial meeting, Korea and the USA aligned themselves with the Japanese site and Russia and China aligned themselves with the European site. No-one budged and a rather laconic ministerial communiqué referred to "two excellent sites for ITER, so excellent in fact that we need further evaluation before making our decisions based on consensus". The ministers agreed to meet again in February but requested that the fusion programme be re-considered with a "broader approach". Since then, there has been a spate of activity on two fronts, one loosely referred to as diplomatic, in which the term has been occasionally stretched enough to test its limits, and the other programmatic, to try to reply to the terms of reference of the ministers, interpreted as meaning finding a large enough second prize and motivating the consensus. The impressive spate of press reports over the last weeks can be consulted at http://fire.pppl.gov .

What is most remarkable is that a project which needs roughly 10 Billion Euro over 25 years has suddenly become so sought after. After years of being too expensive for the richest economies in the world to undertake communally, ITER has graduated to the "must have one" category with not having ITER being considered a disaster. It is not obvious exactly what provoked this sudden transition, although the energy problems, the US R&D priorities and global politics have certainly all contributed. Fusion researchers are now torn between wanting ITER somewhere at all costs and defending the parochial interests of their parties. More sadly, one effect of the 20th December meeting has been a polarisation jeopardising world-wide collaboration, which has previously been such a positive feature of fusion research. We can only hope that by the time of the next ministerial meeting hatchets will have been buried, or lost during the storms. If this is not the case, then ITER runs a serious risk of losing itself after having been so excrutiatingly close to reality—snatching defeat from the jaws of victory to use the well-worn phrase—and that is something from which no party gains. How our energy economy will be altered by fusion over the next 50 years remains under debate, but there is only one way to find out—build ITER.

(for more information on ITER see http://www.iter.org)

noticeboard

2004 Agilent Technologies Europhysics Prize

The Agilent Technologies Europhysics Prize Selection Committee met in Geneva on 23 January. It considered over 30 very good nominations from around the world. After excellent preparation by the Committee an diligent examination, it was decided that the 2004 Agilent Technologies Europhysics Prize is awarded to Michel Devoret, Daniel Esteve, J.E. Hans Mooij and Yasunobu Nakamura for the realisation and demonstration of the quantum bit concept based on superconducting circuits.

Secretary General's report

The EPS Executive Committee engaged in another fruitful "Journée de réflexion" in Bratislava (Slovak Republic). The main themes explored by the participants were Membership and Services, Member Societies, and Relations to the World Outside: EPS and its Member Societies. Presentations on the themes were made by the various participants, and at least 2 will be published later in EPN (increasing the number of members, and new paradigms in journal publishing). The actions to be taken range from the printing of a postcard with information on EPS websites, to analysing and organising sessions on how the EPS can help its member National Societies to increase their membership. Strategy sessions are necessary for the Executive Committee to identify and prioritize actions, and to allocate resources for their implentation. They also serve to inform members of the Executive Committee on issues outside their expertise.

The Europhysics Letters Board of Directors has also just finished its first ever Strategy Days. Following reports from all the partners, including D. Jerome, the incoming Editor in Chief, an ambitious programme of action to increase the prestige, visibility and recognition of the journal will be undertaken.

Strategy sessions are to be encouraged. Committees, Divisions and Groups should take a step back from their normal business and look at their objectives, and what steps are necessary to implement them. I don't know where the quote is from, but I think that it's a fair summary: "If you don't know where you're going, you'll probably end up somewhere else!"

EPS HEPP Outreach prize

The EPS HEPP Board is calling for nominations for its Outreach Prize 2004. The prize is intended for outstanding outreach achievements connected to High Energy Physics and/or Particle Astrophysics. The prize can be attributed to a scientist or to a non scientist.

The prize will consist of a diploma specifying the work of the recipient(s), as well as a cash prize of 2,000 CHF to be contributed from the funding of the division.

The diploma will be handed over to the recipient(s) in the EPS General meeting in Bern in July 2005.

Nominations should be send to Prof. Jorma Tuominiemi (Jorma.Tuominiemi@cern.ch) before April 15th, 2004.

World Year of Physics 2005

The Second Preparatory Conference for the World Year of Physics will be held alongside the APS Spring Meeting in Monteral (March 19-20 2004). The programme will focus on activities to be organized during the year, with reports from around the world. The participants will break up into working groups to share their ideas and difficulties in preparing events on topics such as Light Around the World, Physics on the Road, and Publicity for Your WYP Event.

EPS Council

The EPS Council will meet in Mulhouse on March 26-27. The Council will be invited to adopt a new Constitution for the Society, as well as to vote on an increase in the unit fee. All decisions, and the modified Constitution and By-laws will be published in EPN.

The walls are up

The new office building of the EPS is taking form. The concrete has been laid, and now the interior walls are being built. Although it won't be ready in time for the Council meeting, attendees will be invited to visit and view the progress for themselves.

BOOK REVIEWS

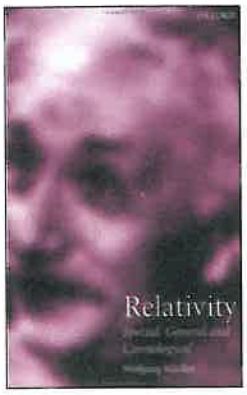

Relativity: Special, General and Cosmological

Wolfgang Rindler
Oxford, 2001
428 pages

Wolfgang Rindler's Relativity: Special, General and Cosmological is intended to be a text readily accessible to advanced undergraduates and beginning graduates. The contents are divided into three sections, as indicated by its title. Prior to these, there is an introduction that prepares the 'Newtonian' reader, by way of providing the necessary motivation and justification, to enter the 'counterintuitive' relativistic arena.

Section I deals specifically with special relativity, and devotes 130 pages, or seven chapters, to its development. All of the material that one would expect to be incorporated in a survey of this length: the Lorentz transformation, relativistic kinematics and mechanics, four-vectors and four-tensors and electromagnetism is lucidly presented.

Section II commences with two chapters on the basic ideas of curvature and metric before embarking on a more detailed exposition of general relativity. The remaining five chapters of this section—some 117 pages—further develop the ideas and concepts introduced in previous chapters. A fairly thorough analysis is carried out of the Schwarzschild spacetime and its physical implications: perihelion precession, deflection of light, gravitational lensing, etc. Black holes are examined, but no further than the Schwarzschild case. A rudimentary discussion on plane gravitational waves is presented to familiarise the reader with the concept of gravity waves. Proceeding on from the penultimate chapter, which finally establishes the full Einstein field equations in conjunction with an analysis of the cosmological constant and deSitter spacetime, the section concludes with some linearised theory.

The third and final section presents an elementary treatise on cosmology. After giving a concise historical account the three remaining chapters (70 pages) are devoted to FRW cosmologies and all the most significant aspects, bearing in mind the length of the section, are highlighted: cosmological redshift, cosmological horizons, the various Friedman models, etc.

The book concludes with a brief appendix that illustrates the procedure for calculating the curvature components for a general 2-, 3-, and 4-dimensional diagonal metric. Exercises are given at the end of each chapter.

My instant impression of the book is one of clarity. A great deal of effort has clearly been lavished on the presentation of each concept, the definitions of quantities and parameters and the illustrative quality of the diagrams. The resolute manner in which Rindler examines sophisticated material in a vivid, revealing way only adds to the work's elegance. The discursive parts that verge on the anecdotal lend the book an air of excitement, compelling the reader further. It was a pleasure to witness the way in which Rindler presented both old and new developments in a most original fashion, including a number of twenty-first century ones. Although I would not emphasise the attributes of any one chapter over another, the section on cosmology will prove highly illuminating for the reader, and the discussion of cosmological horizons is rarely seen in a book of this kind.

I have very few reservations about this book; however, it would certainly benefit by incorporating a bibliography—even though some references are included as footnotes. Furthermore, I would suggest that the book would be more appropriate for an undergraduate audience rather than a postgraduate one. The omission of the Weyl tensor would prohibit any serious study of general relativity at research level. Nevertheless, I recommend that this text should be on the reading list of any undergraduate course in relativity or related areas.

Peter O'Donnell, Anglia Polytechnic University, Cambridge, UK

Books for review

ATOMIC PHYSICS. An exploration through problems and solutions
D. Budker, D.F. Kimball, D.P. DeMille, Oxford University Press, 2004

BEYOND MEASURE. Modern Physics, Philosophy and the Meaning of Quantum Theory
J. Baggott, Oxford, 2004

GAUGE THEORIES IN PARTICLE PHYSICS. Volume II: QCD and the Electroweak Theory. 3rd Edition, I.J.R. Aitchison
A.J.G. Hey, IOP Publishing (Graduate Student Series in Physics), 2004

LASER DIODE MICROSYSTEMS
H. Zappe, Springer, 2004

PROGRESS IN NANO-ELECTRO-OPTICS II. Novel Devices and Atom Manipulation
M. Ohtsu, Springer, 2004

QUANTUM PHYSICS IN ONE DIMENSION
T. Giamarchi, Oxford Science Publications (Int. Series of Monographs on Physics), 2004

RENORMALIZATION METHODS. A guide for beginners
W.D. McComb, Oxford University Press, 2004

SCANNING PROBE MICROSCOPY. The Lab on a Tip
E. Meyer, H.J. Hug, R. Bennewitz, Springer, 2004

SILICON CARBIDE. Recent major advances
W.J. Choyke, H. Matsunami, G. Pensl, Springer, 2004

STRUCTURED FLUIDS. Polymers, Colloids, Surfactants
T.A. Witten, with P.A. Pincus, Oxford, 2004

TOKAMAKS. Third Edition
J. Wesson, Oxford Science Publications (Int. Series of Monographs on Physics), 2004

If you are interested in reviewing books, please send us your name, and contact co-ordinates, along with the your field(s) of specialisation to:

Book Reviews, EPS Secretariat
BP 2136, 68060 Mulhouse Cedex, France

GHMFL

The forthcoming deadline for applications for magnet time allocation (September 2004 to January 2005) at the

GRENOBLE HIGH MAGNETIC FIELD LABORATORY

is **May 28th, 2004**

Scientists of EU countries and Associated States* are entitled to apply under the European Programme to obtain a financial support according to rules defined by the EC. Application forms are available on request.

* Bulgaria, Czech Republic, Republic of Cyprus, Estonia, Hungary, Iceland, Israel, Latvia, Liechtenstein, Lithuania, Norway, Poland, Romania, Slovakia, Slovenia.

Please contact:

E. Mossang
Laboratoire des Champs Magnétiques Intenses,
MPIFKF - CNRS
B.P. 166
38042 Grenoble Cedex 9
FRANCE
Tel. : 33- 4.76.88.74.87
Fax : 33- 4.76.85.56.10
e-mail: mossang@grenoble.cnrs.fr

UNIVERSITÉ DE GENÈVE

The **FACULTY OF SCIENCES** has an opening for a position of

Full or Associate Professor
(Professeur-e ordinaire ou adjoint-e)
in Theoretical Statistical Physics

Responsabilities: this is a full time appointment comprising 6 hours of teaching per week as well as research activities in the area of modern methods and problems in statistical physics.

Degree requirements: Ph.D or equivalent.

Beginning: October 1, 2005 or as agreed.

Applications, including a curriculum vitae, a list of publications and a list of references are to be sent by May 28, 2004 (application deadline extended) to the Dean of the Faculty of Sciences, 30, Quai Ernest Ansermet, CH-1211 Geneva 4 (Switzerland), where further information concerning job description and working conditions can be obtained.

Applications from women are particularly welcomed.

UNIVERSITY OF SOUTHERN DENMARK

www.jobs.sdu.dk

▸ Professor in physics and technology with special duties

The Department of Physics at the University of Southern Denmark in Odense, invites applications for a 5-year employment as professor with special duties with the possibility of another 3-year extension to be filled as soon as possible.

For further information please contact Professor Peter Sigmund, tel. (+45) 6550 3522, e-mail: psi@dou.dk

Applicants should be aware that it is necessary to read the full text for this position before applying. Please find the full notice with further information and address on the University's homepage.

THE LAST DATE FOR APPLICATION: May 3, 2004 at 12:00 hrs.

www.sdu.dk (vacant positions)

SYDDANSKUNIVERSITET.DK